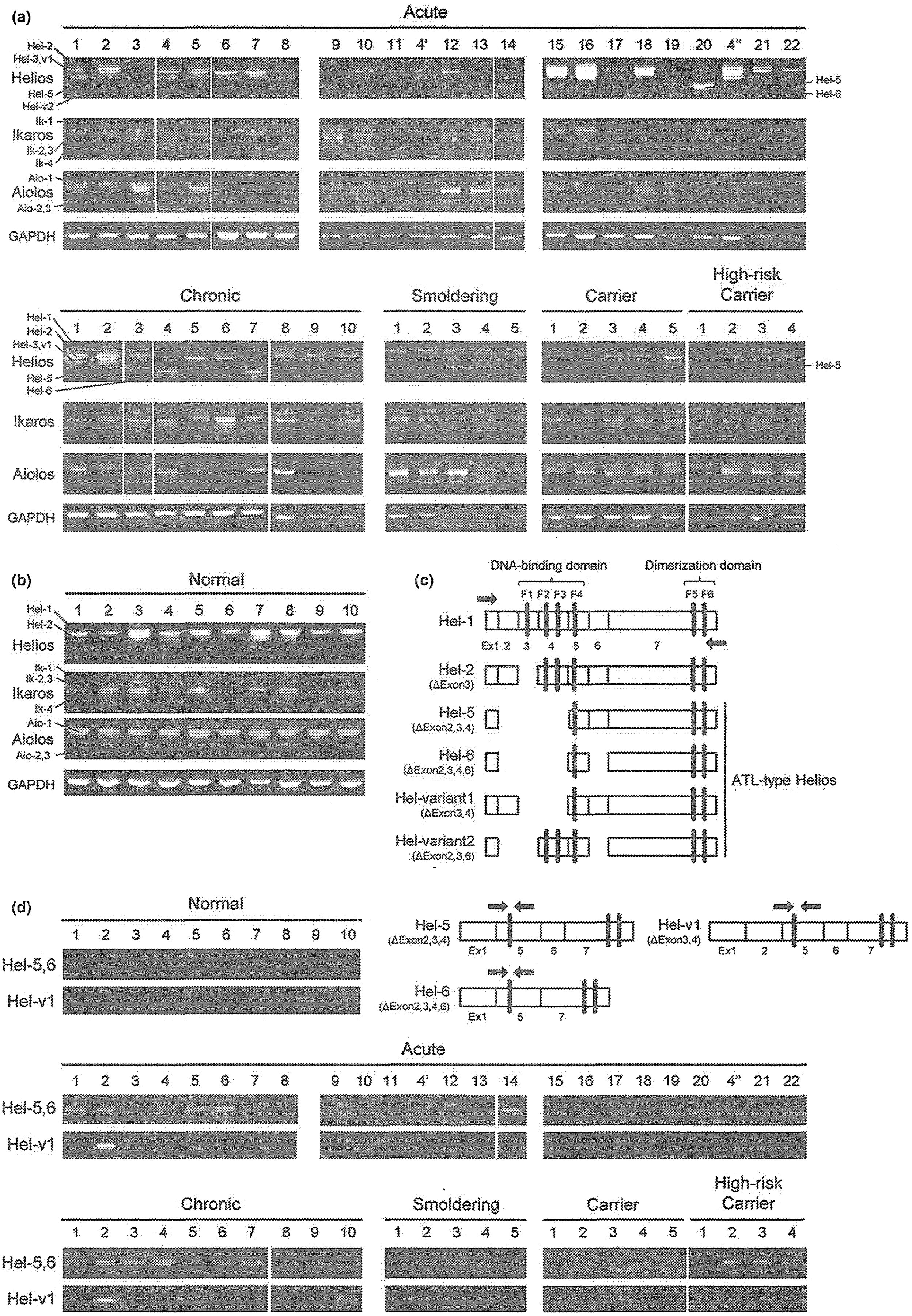
(a)
Acute
1 2 3 4 5 6 7 8 9 10 11 4' 12 13 14 15 16 17 18 19 20 4" 21 22
Hel-2
Hel-3,v1
Helios
Hel-5
Hel-v2
Hel-5
Hel-6
Ik-1
Ikaros
Ik-2,3
Ik-4
Aio-1
Aiolos
Aio-2,3
GAPDH
Chronic
Smoldering
Carrier
High-risk Carrier
1 2 3 4 5 6 7 8 9 10 1 2 3 4 5 1 2 3 4 5 1 2 3 4
Hel-1
Hel-2
Hel-3,v1
Helios
Hel-5
Hel-6
Hel-5
Ikaros
Aiolos
GAPDH
(b)
Normal
1 2 3 4 5 6 7 8 9 10
Hel-1
Hel-2
Helios
Ik-1
Ik-2,3
Ikaros
Ik-4
Aio-1
Aiolos
Aio-2,3
GAPDH
(c)
DNA-binding domain
Dimerization domain
F1 F2 F3 F4
F5 F6
Hel-1
Ex1 2 3 4 5 6 7
Hel-2 (ΔExon3)
Hel-5 (ΔExon2,3,4)
Hel-6 (ΔExon2,3,4,6)
Hel-variant1 (ΔExon3,4)
Hel-variant2 (ΔExon2,3,6)
ATL-type Helios
(d)
Normal
1 2 3 4 5 6 7 8 9 10
Hel-5,6
Hel-v1
Hel-5 (ΔExon2,3,4)
Ex1 5 6 7
Hel-v1 (ΔExon3,4)
Ex1 2 5 6 7
Hel-6 (ΔExon2,3,4,6)
Ex1 5 7
Acute
1 2 3 4 5 6 7 8 9 10 11 4' 12 13 14 15 16 17 18 19 20 4" 21 22
Hel-5,6
Hel-v1
Chronic
Smoldering
Carrier
High-risk Carrier
1 2 3 4 5 6 7 8 9 10 1 2 3 4 5 1 2 3 4 5 1 2 3 4
Hel-5,6
Hel-v1

cellular localization of binding partners. When Hel-6 or Hel-v2 were co-expressed with Hel-1 or Ik-1, they were co-localized in the cytoplasm (Fig. 4b, Fig. S2).

Dominant-negative function of ATL-type Helios isoforms against wild-type Helios and Ikaros. We next examined the functional aspects of these ATL-type Helios isoforms by evaluating their DNA-binding capacities. For EMSA, we used an oligonucleotide probe derived from the promoter region of human *Hes1*, which was a direct target of Ikaros.(34,35) Ectopically expressed Hel-1 or Ik-1 could bind human *Hes1* promoter DNA (Fig. 5a). Supershift assays confirmed the binding specificity (Fig. 5b). In contrast, all ATL-type Helios isoforms did not show any specific binding to the *Hes1* promoter (Fig. 5a). This impossibility of specific DNA binding of ATL-type Helios was confirmed with another independent DNA probe, IkBS4(33,36) (data not shown). In addition, it was found in co-expression experiments that Hel-5 had antagonistic effects on the DNA binding capacity of Ik-1 in a dose-dependent manner (Fig. 5c). Reporter assays showed that Hel-1 and Ik-1 suppressed *Hes1* promoter activity. However, ATL-type Helios isoforms did not show any suppressive activity, and actually slightly activated the promoter (Fig. 5d). Furthermore, they also inhibited the suppressive function of Hel-1 and Ik-1 in a dose-dependent manner (Fig. 5e, Fig. S3). These data clearly indicate that ATL-type Helios isoforms are functionally defective because of a DNA binding deficiency and act dominant-negatively in transcriptional suppression induced by Hel-1 or Ik-1. We also confirmed that Hel-2, which lacks only exon 3 and is a major isoform in ATL cells, did not possess suppressive activity against *Hes1* promoter in spite of having binding activity (Fig. 5a,d).

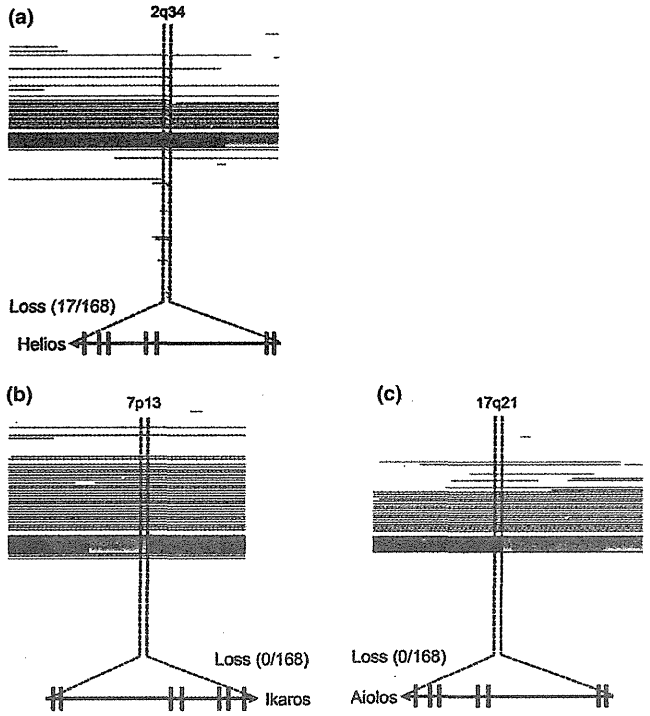

Fig. 2. Genetic abnormalities in *Helios* locus in primary adult T-cell leukemia cells. The results of our copy number analyses(3) (total number, n = 168; acute type, n = 35; chronic type, n = 41; lymphoma type, n = 44; smoldering type, n = 10; intermediate, n = 1; unknown diagnosis, n = 37). Tumor-associated deletion of *Helios* region (17/168) was detected (a). No specific genomic losses were observed in *Ikaros* (b) or *Aiolos* loci (c). Recurrent genetic changes are depicted by horizontal lines based on Copy Number Analyser for GeneChip output of the single nucleotide polymorphism array analysis.

Major ATL-type Helios variant, Hel-5, promotes T cell growth. Given the tumor-suppressive roles of Ikaros family members,(12–15) it was expected that abnormal splicing of Helios could contribute to T cell leukemogenesis. The mRNA level of Helios was significantly downregulated in ATL-related cell lines compared with that in T-cell lines without HTLV-1 (Fig. 6a, Fig. S4). Moreover, Helios protein was not detected in any ATL-derived or HTLV-1-infected cell lines used in this study (Fig. 6b). In contrast, the expression levels of Ikaros mRNA did not show major differences between HTLV-1-infected and uninfected T-cell lines. Those of Aiolos were low in most cell lines irrespective of HTLV-1 infection (Fig. 6a, Fig. S4). Ikaros protein was detected in all T-cell lines used in this study (Fig. 6b). To elucidate the cellular effects of the expression of dominant-negative ATL-type Helios isoforms in T cells, we established stable Jurkat cells expressing Hel-5 (Fig. 6c). A cell proliferation assay confirmed that Hel-5 expression significantly promoted Jurkat cell proliferation

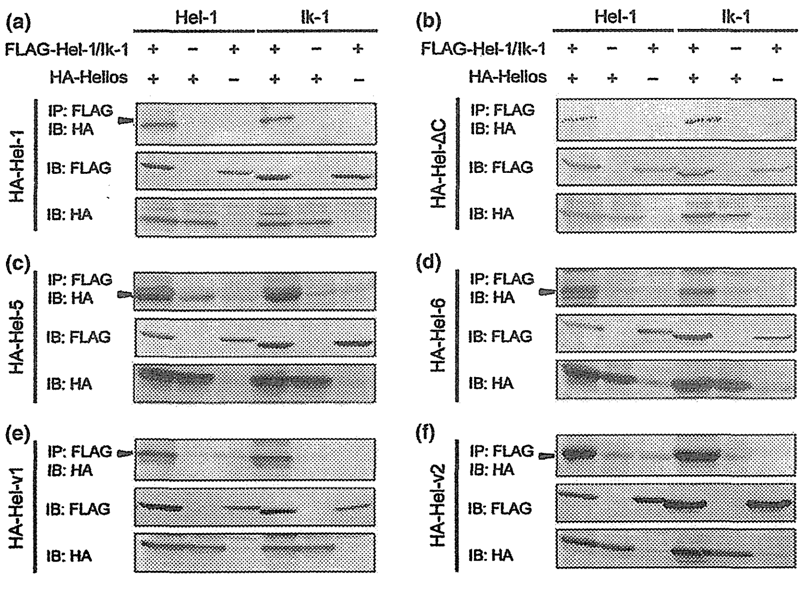

Fig. 3. Dimerization ability of adult T-cell leukemia (ATL)-type Helios isoforms. *In vitro* dimerization assays by co-immunoprecipitation between ATL-type Helios and wild-type Helios or Ikaros proteins. 293T cells were transfected with the indicated combination of expression vectors and subjected to co-immunoprecipitation analyses (top panels). Arrowheads indicate the complex of FLAG and HA-tagged proteins. Middle and bottom panels show the input samples. Hel-1 (a) and Hel-ΔC (b) included as positive and negative controls, respectively. ATL-specific isoforms, Hel-5 (c), Hel-6 (d), Hel-v1 (e), and Hel-v2 (f) were tested. IB, immunoblot; IP, immunoprecipitant.

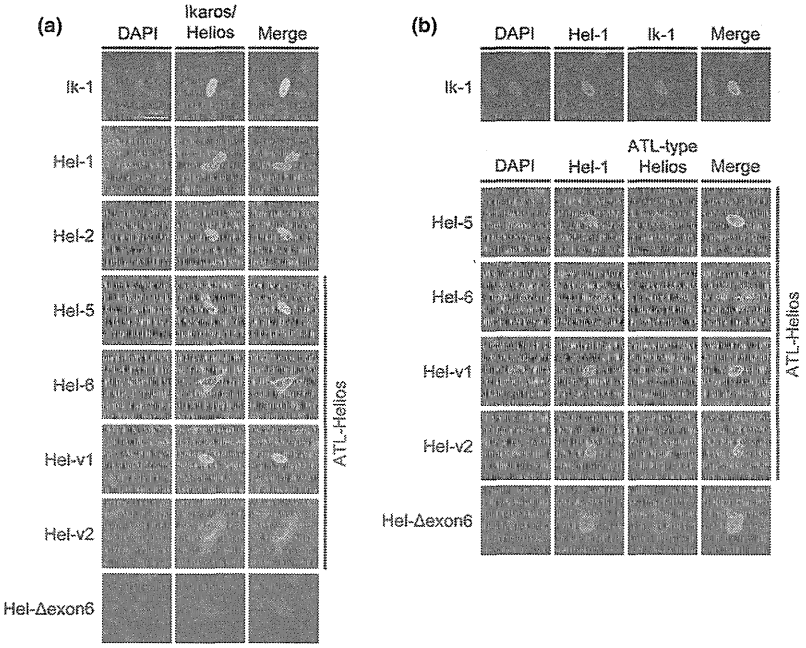

Fig. 4. Subcellular localization of adult T-cell leukemia (ATL)-type Helios isoforms. Immunostaining analyses of Helios and Ikaros proteins. HeLa cells were transfected with each individual expression vector (a) or the indicated combination of expression vectors (b). Each protein was visualized with anti-FLAG (green) or anti-HA antibodies (red). Nuclei were detected by DAPI staining (blue). Colocalization between Ik-1 and ATL-type Helios was shown in Fig. S2. Hel-v1, Hel-variant 1; Hel-v2, Hel-variant 2.

(Fig. 6d). To examine whether the cellular effect of Hel-5 was due to its dominant-negative function against Hel-1 and Ik-1, we carried out further knockdown analyses with specific shRNAs (Fig. 6e). The results showed that knockdown of wild-type Helios or Ikaros led to enhanced cell growth (Fig. 6f), which was consistent with the results of enforced Hel-5 expression. These results collectively suggested that counteraction of Ikaros or Helios by dominant-negative isoforms contributed to T cell growth.

Helios deficiency causes expression of various genes in T cells. We globally searched mRNA expression changes using microarray analysis of Jurkat cells expressing Hel-5 and those of knocked-down Helios or Ikaros (Fig. 7a,b). The results clearly showed differentially expressed gene sets between the transformants and control cells (Fig. 7c). Furthermore, pathway analysis(37) of each upregulated gene set identified activation of several signaling cascades. In particular, we focused on six common pathways identified in both Hel-5 transduced and Helios or Ikaros knocked-down Jurkat cells (Fig. 7d). These pathways are important for various T cell regulations, for example, cell growth, apoptosis resistance, and migration activity. Among these pathways, it has not been reported that the shingosine-1-phosphate (S1P) pathway is regulated by the Ikaros family. We confirmed overexpressed *S1PR1* and *S1PR3*, which are critical receptors for the activation of the S1P pathway, in manipulated Jurkat samples (Fig. 7e).

Discussion

In the present study, on the basis of the integrated analysis of ATL cells using our biomaterial bank in Japan, we revealed a novel molecular characteristic of ATL cells, which is a profound abnormality in the expression of Helios. The abnormal alternative splicing and, in some cases, loss of Helios expression appear to be a part of the basis for advantageous cell growth and survival in ATL cells. We also showed the tumor-suppressive function and target genes, as well as pathways of Helios, in mature human T cells.

Characterization of Ikaros family members revealed profound abnormalities in Helios expression in ATL cells: (i) biased and increased expression of alternatively spliced variants; (ii) suppression of Hel-1 expression; (iii) lack of Helios expression in some cases; and (iv) frequent genomic defects of the *Helios* locus. Our results also revealed that alternatively spliced Helios variants are expressed in PBMCs of HTLV-1 carriers, suggesting that the abnormal splicing of Helios may occur in HTLV-1-infected cells at the carrier state until progression to leukemia development. However, the genomic deletions appear to be one of the important genetic events during the latter stages of leukemia development, as they were observed only in aggressive subtypes of ATL.

The structural characteristics of the ATL-type Helios variants involve a selective lack of one or more zinc fingers in the N-terminal domain. The results of this study indicated that these variant proteins lost DNA binding activity, whereas the capacity of dimerization was preserved. Therefore, these variant proteins hindered transcriptional activities of Ikaros family proteins, showing dominant-negative effects. In addition, a part of ATL-type Helios isoform, which lacks exon 6, is linked to abnormal localization of wild-type Helios and Ikaros. We confirmed that Helios isoforms lacking exon 6 were overexpressed in primary ATL cells (Fig. S5). Interestingly, Hel-2 has reduced transcriptional suppressive activity compared with Hel-1, although it can bind to the target sequence as well as Hel-1. This is similar to a previous report,(36) which noted that the activity of mouse Ik-2 protein for the reporter gene was remarkably lower than that of Ik-1, whereas the binding affinities of Ik-1 and Ik-2 were similar. The exon 3 skip occurred more frequently in ATL cells, compared to PBMCs from normal volunteers (Fig. S6). These results collectively indicate that all abnormalities of Helios expression, including loss of or decreased Hel-1 expression and upregulated Hel-2 and ATL-type Helios, result in abrogation of Ikaros family functions in ATL cells.

We also confirmed that *Hes1*, a target gene of the Notch pathway, is one of the targets of Helios as well as Ikaros.(34,35) A recent study reported that activated Notch signaling may be important to ATL pathogenesis and that Hes1 is upregulated in ATL cells.(38) Thus, we examined expression levels of Hes1 mRNA by quantitative RT-PCR and confirmed the

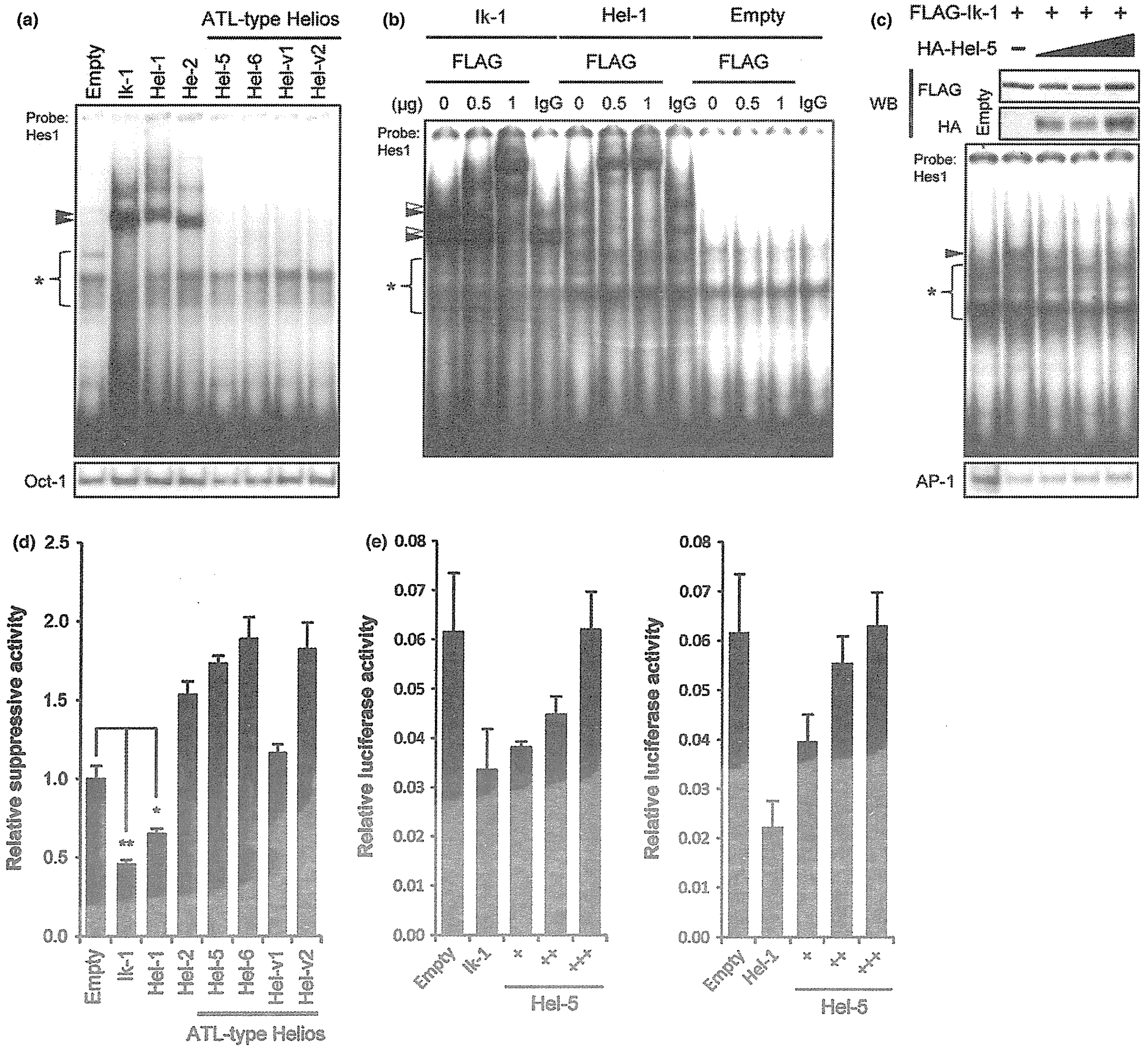

Fig. 5. Dominant-negative function of adult T-cell leukemia (ATL)-type Helios isoforms. (a) DNA-binding activities of wild-type Helios or Ikaros and ATL-type Helios proteins. Each FLAG-tagged Helios or Ikaros isoforms were ectopically expressed in 293T cells and their nuclear extracts were subjected to EMSA with a [γ-^{32}P]-labeled *Hes1* promoter probe. Oct-1 probe was used as an internal control. Arrowheads indicate Helios or Ikaros complexes. *Non-specific bands. Hel-v1, Hel-variant 1; Hel-v2, Hel-variant 2. (b) Results of supershift assays. Anti-FLAG (0, 0.5, 1 μg) or control IgG (1 μg) antibodies were added to each nuclear extract prior to electrophoresis. The black and white arrowheads indicate the supershifted bands of Ik-1 and Hel-1, respectively. (c) Antagonistic effects of Hel-5 on DNA-binding of Ik-1 tested by EMSA. The molar ratios of Ik-1 to Hel-5 plasmids are 1:1, 1:4, and 1:8. Expression levels of FLAG-Ik-1 and HA-Hel-5 were assessed by immunoblotting. The arrowheads indicate the Ik-1 specific band. AP-1 probe was used as an internal control. WB, western blot. (d) Transcriptional suppression activities of various Helios or Ikaros isoforms tested by *Hes1* promoter-luciferase reporter systems ($n = 3$, mean ± SD). Basal *Hes1* promoter activity was defined as firefly/renilla ratio, and suppression activities of Helios or Ikaros are relatively presented. Statistical significance was evaluated by unpaired Student's *t*-test (*$P < 0.05$; **$P < 0.01$). (e) Inhibitory function of Hel-5 against Ik-1 and Hel-1 tested by *Hes1* promoter assay ($n = 3$, mean ± SD). The molar ratios of Ik-1 or Hel-1 to Hel-5 plasmids are 1:1, 1:2, and 1:3. Relative luciferase activities were defined as firefly/renilla ratio.

upregulation in our ATL samples (Fig. S7). Hes1 has been reported to directly promote cell proliferation through the transcriptional repression of p27kip1.(39) Taken together, our results suggest a possibility that abnormalities in Helios expression are one of the causes of Hes1 activation, which may be one of the genetic events involved in ATL leukemogenesis.

Our results show that the Hel-5 variant may have an oncogenic role, whereas the wild-type Helios, Hel-1, shows tumor suppressor-like activity. These findings are consistent with previous findings in mice.(15) Furthermore, our description of expression profiles of stable cells followed by pathway analyses showed activation of several important pathways in lymphocytes for the regulation of proliferation, survival, and others. In particular, we discovered novel molecular cross-talk between the Ikaros family and the S1P pathway. The S1P–S1PR1 axis is known to play important

doi: 10.1111/cas.12181

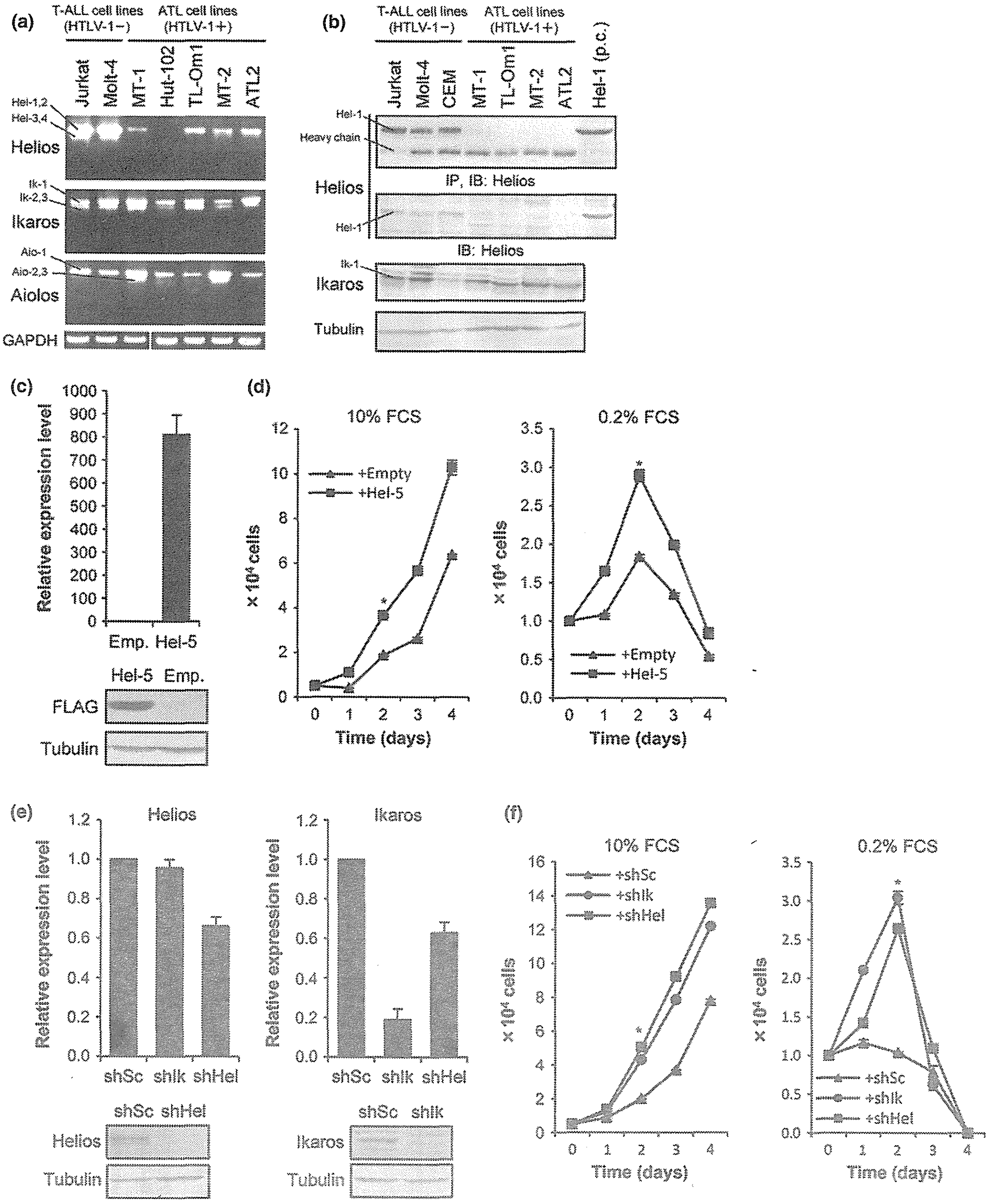

Fig. 6. Hel-5 functions in T cell growth and survival. (a) Expression patterns and levels of Ikaros family genes in various cell lines examined by RT-PCR. ATL, adult T-cell leukemia; T-ALL, acute T lymphoblastic leukemia. (b) Results of immunoblotting analyses of the immunoprecipitants (top panel) and cell lysates (lower panels). Positive control (p.c.), Hel-1 transfectant. IB, immunoblot; IP, immunoprecipitant. (c) Establishment of Jurkat cells stably expressing Hel-5. The Hel-5 level was quantified by quantitative RT-PCR (top, $n = 3$, mean ± SD) and immunoblotting (bottom). (d) Cell proliferation analysis of control cells (▲) and Hel-5-expressing Jurkat cells (■) under two FCS conditions ($n = 3$, mean ± SD). Statistical significance was observed (*$P < 0.01$, Student's t-test). (e) Knockdown analyses of Helios or Ikaros in Jurkat cells. The Helios and Ikaros levels were evaluated by quantitative RT-PCR (top, $n = 3$, mean ± SD) and immunoblotting (bottom), respectively. (f) Cell proliferation curves of scrambled shRNA (shSc) cells (▲), shIkaros (shIk) cells (●), and shHelios (shHel) cells (■) were examined in two FBS conditions ($n = 3$, mean ± SD; *$P < 0.01$).

roles in regulation of the immune system, apoptosis, cell cycle, and migration of lymphocytes.[40–42] Recently, activation of the S1P pathway in various diseases, including leukemia, has been reported, and the therapeutic potential of S1PR1 inhibitors was suggested.[42] Studies of functional roles of S1P pathway activation in ATL cells are now underway in our laboratory.

In conclusion, our present study revealed a novel aspect of molecular abnormalities in ATL cells: a profound deregulation in Helios expression, which appears to play an important role in T-cell proliferation. Our experimental approaches also imply that, in addition to genetic and epigenetic abnormalities, ATL shows abnormal splicing, which has been observed in various human diseases including cancers.[43–45]

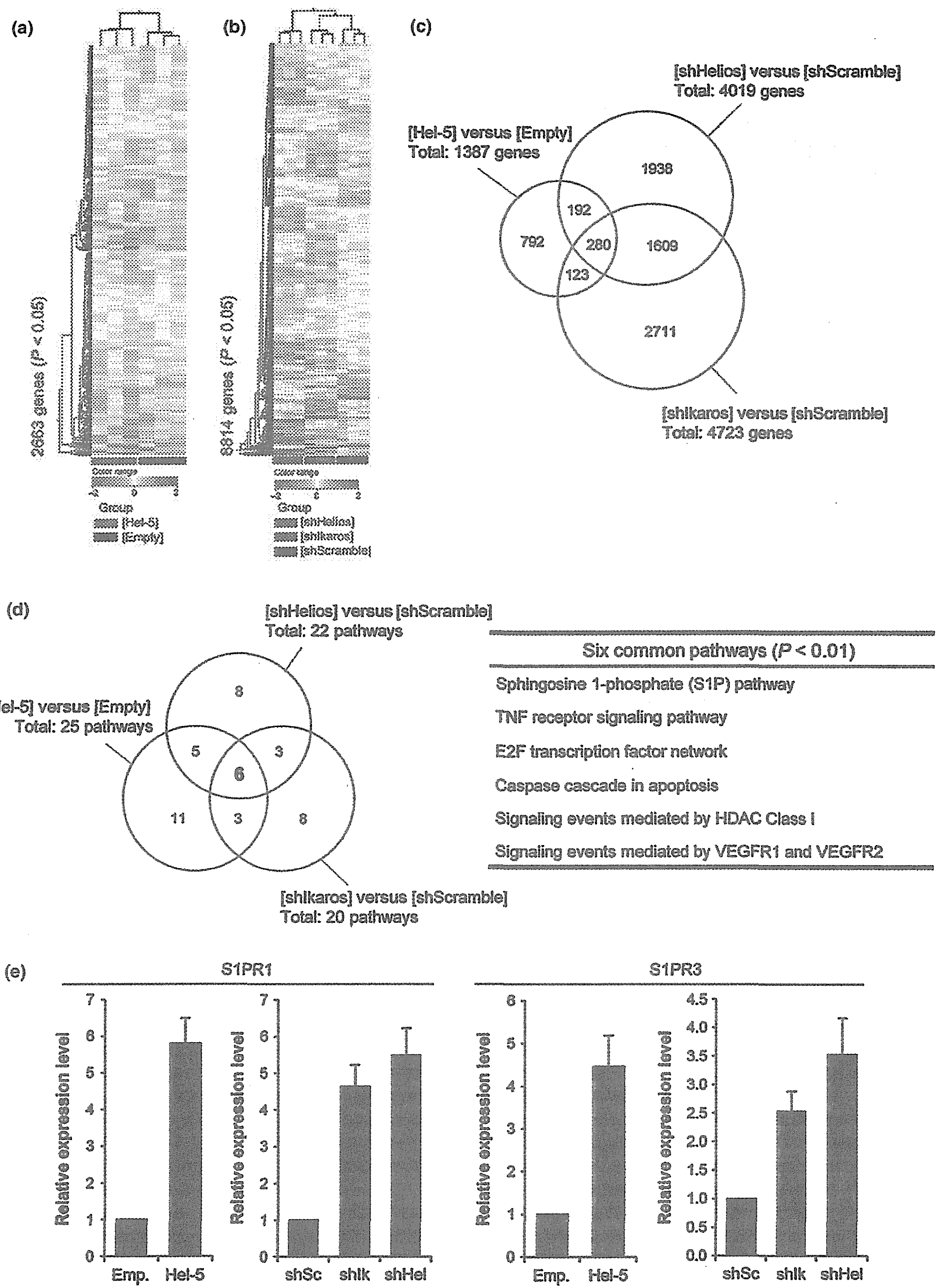

Six common pathways ($P < 0.01$)
Sphingosine 1-phosphate (S1P) pathway
TNF receptor signaling pathway
E2F transcription factor network
Caspase cascade in apoptosis
Signaling events mediated by HDAC Class I
Signaling events mediated by VEGFR1 and VEGFR2

Fig. 7. Comprehensive search for Helios target genes by microarray analysis. (a,b) Gene expression analysis of Jurkat stable cells. The gene expression patterns of Jurkat cells expressing Hel-5 (*n* = 3), shIkaros (*n* = 3), and shHelios (*n* = 3) were comprehensively analyzed by microarray technique. The obtained 2D hierarchical clusters and Pearson's correlation between the cells expressing Hel-5 or not (a) and the cells introducing shHel, shIk, or shSc (b). (c) Venn diagram of differential gene expression pattern in the Jurkat sublines. The each differential expression gene set (5-fold changes, $P < 1 \times 10^{-5}$) was compared. (d) Venn diagram depicting the overlap between the outputs of pathway analysis in Jurkat sublines. The analysis was based on the NCI-Nature Pathway Interaction Database.[37] Each differential pathway set (*t*-test, $P < 0.01$) was compared and the common pathways listed. (e) Results of quantitative RT-PCR of shingosine-1-phosphate receptor 1 (S1PR1) and receptor 3 (S1PR3) in Jurkat sublines (*n* = 3, mean ± SD). HDAC, histone deacetylase; VEGFR, vascular endothelial growth factor receptor.

Acknowledgments

We thank Mr. M. Nakashima and Ms. T. Akashi for support and maintenance of the Joint Study on Prognostic Factors of ATL Development. This work is supported by JSPS KAKENHI Grant Numbers 24790436 (M.Y.), 23390250 (T.W.), 23659484 (T.W.), 23 6291 (S.A.), NEXT KAKENHI Grant Number 221S0001 (T.W.), and a Grant-in-Aid from the Ministry of Health, Labor and Welfare of Japan H24-G-004 (M.Y. and T.W.).

Disclosure Statement

The authors have no conflict of interest.

References

1 Yamaguchi K. Watanabe T. Human T lymphotropic virus type-I and adult T-cell leukemia in Japan. *Int J Hematol* 2002; **76**: 240–45.

2 Iwanaga M. Watanabe T, Utsunomiya A *et al.* Human T-cell leukemia virus type I (HTLV-1) proviral load and disease progression in asymptomatic HTLV-1 carriers: a nationwide prospective study in Japan. *Blood* 2010; **116**: 1211–19.

3 Yamagishi M, Nakano K, Miyake A *et al.* Polycomb-mediated loss of miR-31 activates NIK-dependent NF-κB pathway in adult T cell leukemia and other cancers. *Cancer Cell* 2012; **21**: 121–35.

4 Yamagishi M. Watanabe T. Molecular hallmarks of adult T cell leukemia. *Front Microbiol* 2012; **3**: 334.

5 Lo K. Landau NR, Smale ST. LyF-1, a transcriptional regulator that interacts with a novel class of promoters for lymphocyte-specific genes. *Mol Cell Biol* 1991; **11**: 5229–43.

6 Georgopoulos K, Moore DD, Derfler B. Ikaros, an early lymphoid-specific-transcription factor and a putative mediator for T cell commitment. *Science* 1992; **258**: 808–12.

7 Hahm K. Ernst P, Lo K. Kim GS. Turck C, Smale ST. The lymphoid transcription factor LyF-1 is encoded by specific, alternatively spliced mRNAs derived from the Ikaros gene. *Mol Cell Biol* 1994; **14**: 7111–23.

8 Sun L, Liu A. Zinc finger-mediated protein interactions modulate Ikaros activity, a molecular control of lymphocyte development. *EMBO J* 1996; **15**: 5358–69.

9 Morgan B, Sun L, Avitahl N *et al.* Aiolos, a lymphoid restricted transcription factor that interacts with Ikaros to regulate lymphocyte differentiation. *EMBO J* 1997; **16**: 2004–13.

10 Kelley CM, Ikeda T, Koipally J *et al.* Helios, a novel dimerization partner of Ikaros expressed in the earliest hematopoietic progenitors. *Curr Biol* 1998; **8**: 508–15.

11 Cobb BS. McCarty AS, Brown KE *et al.* Helios, a T cell-restricted Ikaros family member that quantitatively associates with Ikaros at centromeric heterochromatin. *Genes Dev* 1998; **12**: 782–96.

12 Winandy S, Wu P, Georgopoulos K. A dominant mutation in the Ikaros gene leads to rapid development of leukemia and lymphoma. *Cell* 1995; **83**: 289–99.

13 Wang JH, Nichogiannopoulou A, Wu L *et al.* Selective defects in the development of the fetal and adult lymphoid system in mice with an Ikaros null mutation. *Immunity* 1996; **5**: 537–49.

14 Wang JH, Avitahl N, Cariappa A *et al.* Aiolos regulates B cell activation and maturation to effector state. *Immunity* 1998; **9**: 543–53.

15 Zhang Z, Swindle CS, Bates JT. Ko R, Cotta CV, Klug CA. Expression of a non-DNA-binding isoform of Helios induces T-cell lymphoma in mice. *Blood* 2007; **109**: 2190–7.

16 Sun L, Crotty ML, Sensel M *et al.* Expression of dominant-negative Ikaros isoforms in T-cell acute lymphoblastic leukemia. *Clin Cancer Res* 1999; **5**: 2112–20.

17 Nakase K, Ishimaru F, Avitahl N *et al.* Dominant negative isoform of the Ikaros gene in patients with adult B-cell acute lymphoblastic leukemia. *Cancer Res* 2000: **60**: 062–4065.

18 Takanashi M, Yagi T, Imamura T *et al.* Expression of the Ikaros gene family in childhood acute lymphoblastic leukaemia. *Br J Haematol* 2002; **117**: 525–30.

19 Nishii K. Katayama N, Miwa H. Non-DNA-binding Ikaros isoform gene expressed in adult B-precursor acute lymphoblastic leukemia. *Leukemia* 2002; **16**: 1285–92.

20 Tonnelle C. Imbert M-C, Sainty D, Granjeaud S, N'Guyen C, Chabannon C. Overexpression of dominant-negative Ikaros 6 protein is restricted to a subset of B common adult acute lymphoblastic leukemias that express high levels of the CD34 antigen. *Hematol J* 2003; **4**: 104–9.

21 Klein F, Feldhahn N, Herzog S *et al.* BCR-ABL1 induces aberrant splicing of IKAROS and lineage infidelity in pre-B lymphoblastic leukemia cells. *Oncogene* 2006; **25**: 1118–24.

22 Zhou F, Mei H, Jin R. Li X. Chen X. Expression of ikaros isoform 6 in chinese children with acute lymphoblastic leukemia. *J Pediatr Hematol Oncol* 2011; **33**: 429–32.

23 Mullighan CG. Miller CB, Radtke I *et al.* BCR-ABL1 lymphoblastic leukaemia is characterized by the deletion of Ikaros. *Nature* 2008; **453**: 110–14.

24 Kano G, Morimoto A. Takanashi M *et al.* Ikaros dominant negative isoform (Ik6) induces IL-3-independent survival of murine pro-B lymphocytes by activating JAK-STAT and up-regulating Bcl-xl levels. *Leuk Lymphoma* 2008; **49**: 965–73.

25 Iacobucci I. Lonetti A, Messa F *et al.* Expression of spliced oncogenic Ikaros isoforms in Philadelphia-positive acute lymphoblastic leukemia patients treated with tyrosine kinase inhibitors: implications for a new mechanism of resistance. *Blood* 2008; **112**: 3847–55.

26 Mullighan CG. Su X, Zhang J *et al.* Deletion of IKZF1 and prognosis in acute lymphoblastic leukemia. *N Engl J Med* 2009; **360**: 470–80.

27 Kuiper RP, Waanders E, van der Velden VHJ *et al.* IKZF1 deletions predict relapse in uniformly treated pediatric precursor B-ALL. *Leukemia* 2010; **24**: 1258–64.

28 Nakase K, Ishimaru F. Fujii K *et al.* Overexpression of novel short isoforms of Helios in a patient with T-cell acute lymphoblastic leukemia. *Exp Hematol* 2002; **30**: 313–17.

29 Fujii K, Ishimaru F, Tabayashi T *et al.* Over-expression of short isoforms of Helios in patients with adult T-cell leukaemia/lymphoma. *Br J Haematol* 2003; **120**: 986–9.

30 Fujiwara SI, Yamashita Y, Nakamura N *et al.* High-resolution analysis of chromosome copy number alterations in angioimmunoblastic T-cell lymphoma and peripheral T-cell lymphoma, unspecified, with single nucleotide polymorphism-typing microarrays. *Leukemia* 2008; **22**: 1891–8.

31 Fujimoto R, Ozawa T. Itoyama T, Sadamori N, Kurosawa N, Isobe M. HELIOS-BCL11B fusion gene involvement in a t(2;14)(q34;q32) in an adult T-cell leukemia patient. *Cancer Genet* 2012; **205**: 356–64.

32 Shimoyama M. Diagnostic criteria and classification of clinical subtypes of adult T-cell leukaemia-lymphoma. A report from the Lymphoma Study Group (1984–87). *Br J Haematol* 1991; **79**: 428–37.

33 Tabayashi T. Ishimaru F, Takata M *et al.* Characterization of the short isoform of Helios overexpressed in patients with T-cell malignancies. *Cancer Sci* 2007; **98**: 182–8.

34 Kathrein KL, Chari S, Winandy S. Ikaros directly represses the notch target gene Hes1 in a leukemia T cell line: implications for CD4 regulation. *J Biol Chem* 2008; **283**: 10476–84.

35 Kleinmann E. Geimer Le Lay AS. Sellars M, Kastner P, Chan S. Ikaros represses the transcriptional response to Notch signaling in T-cell development. *Mol Cell Biol* 2008; **28**: 7465–75.

36 Molnár A, Georgopoulos K. The Ikaros gene encodes a family of functionally diverse zinc finger DNA-binding proteins. *Mol Cell Biol* 1994; **14**: 8292–303.

37 Schaefer CF. Anthony K. Krupa S *et al.* PID: the pathway interaction database. *Nucleic Acids Res* 2009; **37**: D674–9.

38 Pancewicz J, Taylor JM, Datta A. Notch signaling contributes to proliferation and tumor formation of human T-cell leukemia virus type 1-associated adult T-cell leukemia. *Proc Natl Acad Sci USA* 2010; **107**: 16619–24.

39 Murata K. Hattori M, Hirai N *et al.* Hes1 directly controls cell proliferation through the transcriptional repression of p27Kip1. *Mol Cell Biol* 2005; **25**: 4262–71.

40 Maeda Y, Seki N, Sato N, Sugahara K. Chiba K. Sphingosine 1-phosphate receptor type 1 regulates egress of mature T cells from mouse bone marrow. *Int Immunol* 2010; **22**: 515–25.

41 Spiegel S, Milstien S. The outs and the ins of sphingosine-1-phosphate in immunity. *Nat Rev Immunol* 2011; **11**: 403–15.

42 Maceyka M, Harikumar KB, Milstien S. Spiegel S. Sphingosine-1-phosphate signaling and its role in disease. *Trends Cell Biol* 2012; **22**: 50–60.

43 Ghigna C. Valacca C, Biamonti G. Alternative splicing and tumor progression. *Curr Genomics* 2008; **9**: 556–70.

44 David CJ, Manley JL. Alternative pre-mRNA splicing regulation in cancer: pathways and programs unhinged. *Genes Dev* 2010; **24**: 2343–64.

45 Blair CA. Zi X. Potential molecular targeting of splice variants for cancer treatment. *Indian J Exp Biol* 2011; **49**: 836–9.

Supporting Information

Additional Supporting Information may be found in the online version of this article:

Fig. S1. Deregulated expression of Ikaros family genes in primary adult T-cell leukemia cells.

Fig. S2. Colocalization of wild-type Ikaros and adult T-cell leukemia-type Helios.

Fig. S3. Dominant-negative inhibition of Hel-6, Hel-v1, and Hel-v2 in the suppressive activities of wild-type Helios and Ikaros.

Fig. S4. Downregulation of the expression of Helios mRNA in HTLV-1-positive T cell lines.

Fig. S5. Overexpression of abnormal Helios isoforms lacking exon 6 in adult T-cell leukemia samples.

Fig. S6. Relative value of Helios transcripts skipping exon 3 to all is upregulated in primary adult T-cell leukemia cells.

Fig. S7. Upregulated expression of Hes1 in primary adult T-cell leukemia cells.

Table S1. Clinical characteristics of adult T-cell leukemia patients and HTLV-1 carriers.

Table S2. Primer list and probe sequences.

doi: 10.1111/cas.12181

ELSEVIER

CrossMark

Institut Pasteur

Microbes and Infection 15 (2013) 491–505

www.elsevier.com/locate/micinf

Original article

Viral interference with host mRNA surveillance, the nonsense-mediated mRNA decay (NMD) pathway, through a new function of HTLV-1 Rex: implications for retroviral replication

Kazumi Nakano [a], Tomomi Ando [a,b], Makoto Yamagishi [a], Koichi Yokoyama [a], Takaomi Ishida [c], Takeo Ohsugi [d], Yuetsu Tanaka [e], David W. Brighty [f], Toshiki Watanabe [a,*]

[a] *Laboratory of Tumor Cell Biology, Department of Medical Genome Sciences, Graduate School of Frontier Sciences, The University of Tokyo, 4-6-1, Shirokanedai, Minatoku, Tokyo 108-8639, Japan*
[b] *Department of Virology II, National Institute of Infectious Diseases, 1-23-1, Toyama, Shinjukuku, Tokyo 162-8640, Japan*
[c] *Research Center for Asian Infectious Diseases, The Institute of Medical Science, The University of Tokyo, 4-6-1, Shirokanedai, Minatoku, Tokyo 108-8639, Japan*
[d] *Center for Animal Resources and Development, The University of Kumamoto, 2-2-1, Honsho, Kumamoto 860-0811, Japan*
[e] *Department of Immunology, Graduate School of Medicine, University of the Ryukyus, 207 Uehara, Nishihara-cho, Nakagusuku, Okinawa 903-0215, Japan*
[f] *Division of Cancer Research, Medical Research Institute, University of Dundee, Scotland DD1 9SY, UK*

Received 9 January 2013; accepted 18 March 2013
Available online 27 March 2013

Abstract

Nonsense-mediated mRNA decay (NMD) is an essential and conserved cellular mRNA quality control mechanism. RNA signals to express viral genes from overlapping open reading frames potentially initiate NMD, nevertheless it is not clear whether viral RNAs are sensitive to NMD or if viruses have evolved mechanisms to evade NMD. Here we demonstrate that the genomic and full-length mRNAs of Human-T-cell Leukemia Virus type-I (HTLV-1), a retrovirus responsible for Adult T-cell Leukemia (ATL), are sensitive to NMD. They exhibit accelerated turnover in NMD-activated cells, while siRNA-mediated knockdown of NMD-master-regulator, UPF1, promotes enhanced stability of them. These effects on RNA stability were recapitulated by a reporter construct encoding the HTLV-1 translational frameshift signal of *gag-pol*. In agreement with the RNA stability, viral protein expression from the integrated provirus was inversely correlated with cellular NMD activity. We further demonstrated that the viral RNA-binding protein, Rex, approves the stability of viral RNA by inhibiting NMD. Significantly, Rex establishes a general block to NMD, as both NMD-responsive reporter transcripts and natural host-encoded NMD substrates were stabilized in the presence of Rex. Thus, we suggest that Rex not only stabilizes viral transcripts, but also perturbs cellular mRNA metabolism and host cell homeostasis via inhibition of NMD.

Keywords: HTLV-1; HTLV-1 Rex; NMD; Retroviral genomic RNA; Host–pathogen interaction

---

1. Introduction

Nonsense-mediated mRNA decay (NMD) is an mRNA surveillance mechanism that is conserved in eukaryotic cells. The degradation of aberrant mRNAs containing premature termination codons (PTCs) is the most studied NMD function. Positioned upstream of the natural end of open reading frames (ORFs), PTCs are stop codons that arise from frameshifts due to mutations or aberrant mRNA processing events. Truncated proteins encoded by such abnormal mRNAs are often deleterious to cells because they may be structurally unstable and result in translation product aggregation or may function as dominant negative inhibitors of wild-type (WT) protein function [1]. Recently, it has been recognized that NMD function is important for eliminating aberrant mRNAs and

---

* Corresponding author. Tel.: +81 3 5449 5298; fax: +81 3 5449 5418.
E-mail addresses: tnabe@ims.u-tokyo.ac.jp, tnabe@k.u-tokyo.ac.jp (T. Watanabe).

http://dx.doi.org/10.1016/j.micinf.2013.03.006

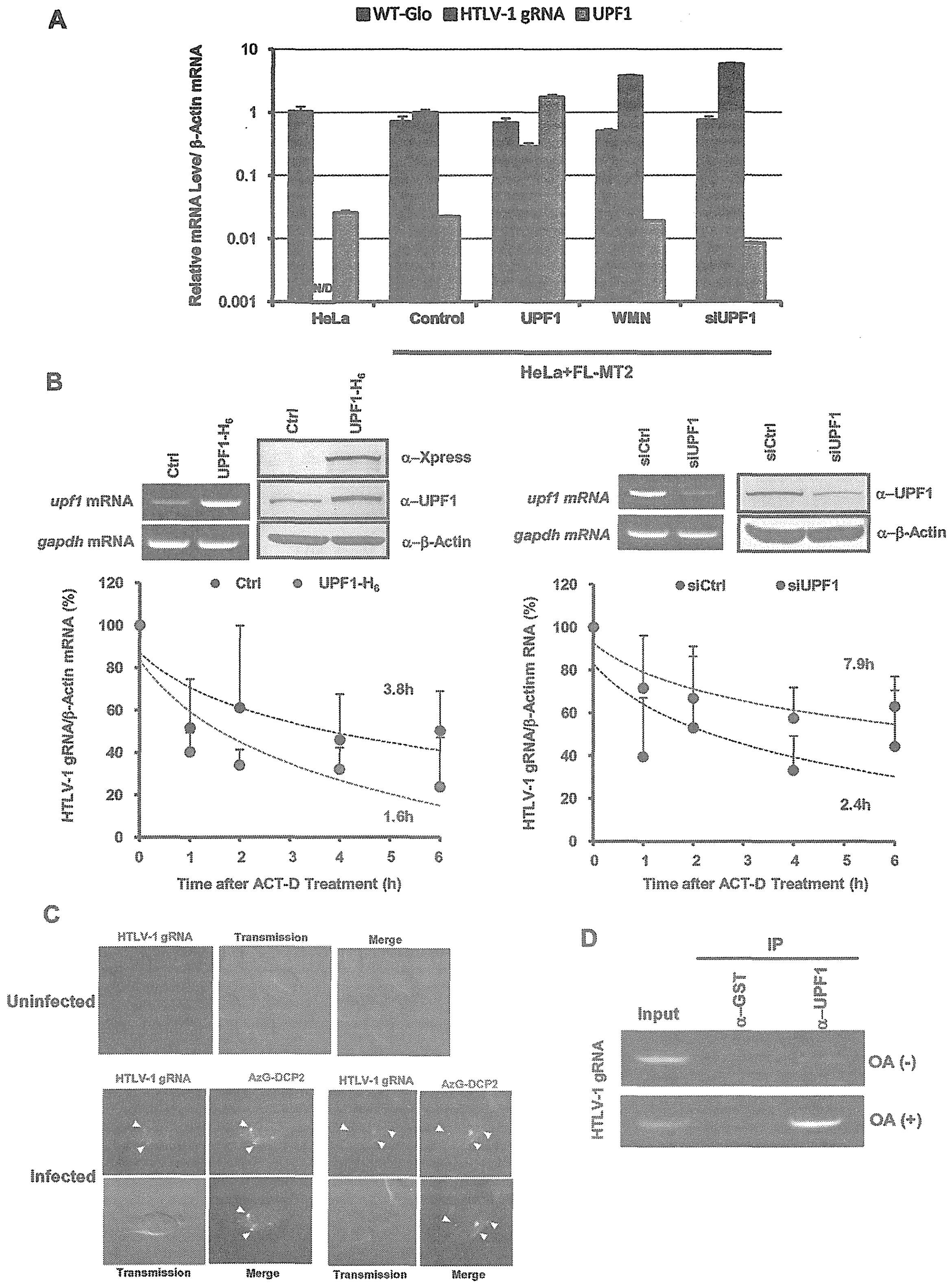

Fig. 1. HTLV-1 genomic unspliced RNA is a NMD target. (A) Changes in the cellular level of HTLV-1 unspliced mRNA were dependent on cellular NMD activity. The steady-state level of HTLV-1 genomic primary transcripts (HTLV-1 gRNA) accumulating from the pFL-MT2 infectious clone in HeLa cells was decreased by UPF1 overexpression and increased by NMD inhibition through siUPF1 transfection or wortmannin treatment. By contrast, the level of WT-β-globin mRNA (WT-Glo), which is not a NMD target, was not influenced by the cellular level of UPF1 or wortmannin treatment, indicating that the level of HTLV-1 genomic mRNA is selectively influenced by cellular NMD activity. (B) UPF1-dependent HTLV-1 genomic mRNA instability in HTLV-1 infected HeLa cells by co-cultivation with

controlling the expression levels of a considerable number of normal cellular mRNAs that possess NMD-activating structures, such as uORFs and introns within the 3′ untranslated region (UTR) [2]. The NMD machinery achieves these functions by coupling with the splicing and translational machinery [3,4]. Thus, NMD is an essential mechanism that governs mRNA quality and quantity in eukaryotic cells.

RNA viruses have compact genomes, but they have evolved elegant mechanisms to maximize coding potential and precisely regulate the expression of encoded genes. Overlapping reading frames, internal ribosome entry sites, alternative splicing, suboptimal Kozak sequences, and ribosomal frameshifting are among the varied mechanisms used to maximize genomic coding potential and regulate viral gene expression [5]. The presence of such signals in cellular mRNA is unusual, but wherever they occur, there is significant potential to activate the NMD pathway, which destabilizes RNA and increases mRNA turnover [6–8]. Programmed Ribosomal Frameshift (PRF) is a mechanism frequently used by viruses to alter the translational reading frame by shifting the ribosome at a frameshifting sequence often referred to as a "slippery site" [9]. Especially, *pgk1* mRNA stability assays with or without L-A viral −PRF signal showed that −PRF itself functioned as *cic*-acting destabilization element through NMD [7]. In addition, as many as one-third of all cellular mRNA variants produced by alternative splicing are reported to be potential targets of NMD [6,8]. As reviewed by Dickson and Wilusz [10], virus–host mRNA surveillance interface is attracting growing interest as a new aspect of host–pathogen interactions. Nevertheless, viral mechanisms to evade host mRNA surveillance to protect its own RNA has been mostly left uninvestigated. Accumulated knowledge indicates that viruses have various strategies to avoid or incapacitate host mRNA decay. Therefore, for RNA viruses, there are important unresolved questions. First, are RNA viruses that possess overlapping reading frames, alternative stop codons, and translational frameshift sequences sensitive to NMD? If so, do RNA viruses actively avoid the NMD surveillance pathway? Finally, are viral factors required for evasion of host-encoded NMD?

The human T-cell leukemia virus type I (HTLV-1) is a delta retrovirus that causes aggressive adult T-cell leukemia (ATL) in some infected individuals. The genomic RNA of this retrovirus encodes more than ten ORFs with associated stop codons within a full-length genomic RNA of 8685 nucleotides. HTLV-1 employs a number of mechanisms to achieve appropriate and ordered expression of these genes, including alternative splicing and PRF. In particular, Gag, Pro, and Pol, is translationally regulated by in-frame read-through and two −1 PRF signals at 1718 and 2245 nucleotides, respectively. In addition, the HTLV-1 genomic RNA contains two major splice sites. Unspliced HTLV-1 RNA yields Gag, Pro, and Pol proteins, singly spliced RNA produces Env, while the functional proteins derived from the pX region can be translated only from double-spliced mRNA. Therefore, we hypothesized that because of the unusual structure and processing signals, which include multiple stop codons, translational frameshifts, and a downstream splice acceptor site, the full-length HTLV-1 genomic RNA and *gag/pol* mRNA appear to be prime candidates for interference with viral mRNA accumulation via NMD.

Here we explored whether the presence of multiple stop codons and −1 PRF signals in HTLV-1 viral transcripts activates the host NMD. Also, we investigated how such viral RNA survives in the face of a highly efficient cellular mRNA quality control system.

2. Materials and methods

2.1. NMD reporter constructs and assays

To measure overall cellular NMD activity, we constructed NMD reporter plasmids based on widely used β-globin as well as on a HTLV-1 *gag* mRNA fragment. The β-globin-based NMD reporter plasmid was created based on Boelz et al. [11] with modification dependent on the type of experiment. Detailed methods of reporter construction and luciferase assays are available in Supplementary material.

2.2. HTLV-1 expression in HeLa cells

To express HTLV-1 in HeLa cells, transfection of an infectious clone (pFL-MT2) [12] (for Fig. 1A) or co-cultivation with MT-2 (for Fig. 1B–D, 3C–E, 6B–D) was employed. Please see Supplementary material for more detail.

2.3. Inhibition of UPF1 and UPF2

The siRNA sequences against *upf1* mRNA and *upf2* mRNA are described elsewhere [13,14]. The sequence of the control siRNA was 5′-AGGUCGAACUACGGGUCAA(TT)-3′. Wortmannin is a PI3K inhibitor and known to inhibit UPF1 activity by inhibiting SMG1, the kinase of UPF1. For complete inhibition of UPF1 activity, cells were treated with 100 μM wortmannin for 19–20 h before sampling. For construction of

MT-2 cells. The stability of HTLV-1 genomic mRNA decreased in the cells overexpressing His-tagged UPF1 (UPF1-H_6) (half-life = 1.6 h) compared with control (Ctrl) cells transfected with the empty vector (half-life = 3.8 h). In contrast, the stability of HTLV-1 genomic mRNA in cells transfected with siUPF1 (half-life = 7.9 h) increased compared with that in cells transfected with the control siRNA (siCtrl) (half-life = 2.4 h). The half-life was calculated based on the regression curve (dashed line). Above each graph, semi-quantitative RT-PCR analysis of relative RNA levels (left panel) and Western blotting analysis of protein levels (right panel) are shown ($n = 4$, mean ± SE). (C) HTLV-1 genomic RNA, detected by in situ hybridization with the *gag/pol* cDNA probe in HTLV-1 infected HeLa cells, co-localized with AzamiGreen-DCP2, a P-body marker, indicating that a notable fraction of HTLV-1 genomic unspliced RNA (gRNA) accumulates in P-bodies. No clear signals in negative control HeLa cells without infection confirmed that the *gag/pol* cDNA probe specifically detected gRNA in infected HeLa cells. (D) Interaction between UPF1 and HTLV-1 unspliced mRNA. HTLV-1 genomic unspliced mRNA was found in the UPF1 complex co-immunoprecipitated with anti-UPF1 antibody from whole-cell lysate of MT-2 cells (top panel). Moreover, sustained phosphorylation of UPF1 through okadaic acid (OA) treatment increased the level of bound HTLV-1 genomic mRNA recovered (bottom panel).

an antisense (As)-*upf2* mRNA-expressing plasmid and suppression of UPF2, please see Supplementary material.

2.4. Measurement of mRNA stability

First, the cells (3×10^5/mL) were resuspended in culture medium, and 1.5×10^5/500 μL of the cells were sampled as the 0 h sample. Second, the culture medium was replaced by that containing actinomycin D (5 μg/mL) and seeded at 1.5×10^5/500 μL in 5 wells of a 12-well plate. The cells were sampled 1, 2, 3, 4, and/or 6 h after the addition of actinomycin D to each well, and total RNA was extracted using Isogen (Nippon Gene Co., Ltd.) for the measurement of mRNA levels by real-time PCR. The levels of NMD target mRNAs (MAP3K14, IL6, DUSP10, Fyn, PTPRF, ARHGEF18, ASNS, and DEXI) were measured at each time point and standardized by the corresponding β-actin mRNA level, which is not a NMD target. Methods in establishment of CEM cells, which stably overexpress Rex protein are available in Supplementary material.

2.5. Protein expression plasmids

The UPF1 expression plasmid was constructed by inserting the full-length cDNA fragment of human *upf1* into the *Eco*RI site of pCDNA3.1/His C (Invitrogen) for His/Xpress-UPF1 expression. The expression plasmids of HTLV-1 regulatory proteins were constructed by inserting the PCR-amplified cDNA fragments of HTLV-1 *rex*, *tax*, *p30ii*, *p12*, *p13*, and *hbz* from a cDNA pool derived from MT-2 cells at the *XhoI*/*SpeI* sites of pME-FLAG for FLAG-tagged proteins. The *dcp2* cDNA fragment was inserted at the *Bam*HI site of pmAG1-MN1 (Amalgaam Co., Ltd.) for AzamiGreen-tagged DCP2 expression.

2.6. Quantitative and semi-quantitative RT-PCR and genomic DNA PCR

The levels of viral and host cell transcripts were measured by quantitative or semi-quantitative RT-PCR. Total RNA was extracted using Isogen (Nippon Gene Co., Ltd.) following the manufacturer's protocol. DNase I treatment was performed to eliminate genomic DNA contamination. Extracted total RNA samples were subjected to reverse transcription using SuperScript II (Invitrogen), followed by quantitative real-time PCR using SYBR Premix Ex Taq (Takara Bio Inc.) and thermal cycler dice (Takara) or by semi-quantitative PCR. The sequences of primers used for PCR are available in Supplementary material.

2.7. Western blotting and antibodies

For the Western blotting of HTLV-1 Tax, a monoclonal Tax antibody (LT-4) was used [15]. Rex antibody, used in Western blotting for the HTLV-1 Rex protein, was monoclonal rat antiserum (Tanaka, unpublished data), while HTLV-1 Gag-p19 and Gag-p24 antibodies were the monoclonal mouse antibodies, GIN-7 and NOR-1, respectively [16]. The following primary antibodies were purchased from the indicated companies: hUPF1 (#9435; Cell Signaling Technology Inc.), hUPF2 (ab28712-200; Abcam), FLAG (F3165; Sigma–Aldrich Corporation), GST (#27-4577-01; GE Healthcare Bioscience), Xpress (46-0528; Invitrogen), β-actin (sc-69879; Santa Cruz Biotechnology, Inc.). For the secondary antibodies conjugated with alkaline phosphatase, anti-mouse IgG (S372B; Promega), anti-rabbit IgG (S373B; Promega), or anti-goat IgG (V115A; Promega) was used depending on the host species of the primary antibody.

2.8. Indirect immunofluorescence in situ RNA hybridization assays

HeLa cells transiently expressing AzamiGreen-DCP2 was co-cultured with MT-2 at 37 °C for 24 h to express HTLV-1. MT-2 cells were removed by washing 3 times with PBS, then the infected HeLa cells were further incubated at 37 °C for 24 h. In situ hybridization of HTLV-1 unspliced mRNA was performed by incubating the fixed and permeabilized cells with DIG-labeled HTLV-1 *gag*/*pol* cDNA probes at 37 °C for 16 h. The hybridized probes were detected by immunocytochemistry using rhodamine-conjugated anti-DIG antibody (Roche). The subcellular localization of HTLV-1 unspliced mRNA and AzamiGreen-DCP2 was observed using a confocal laser scanning microscope (LSM510; Carl Zeiss AG). As negative control, HeLa cells without HTLV-1 infection were also subjected to the same hybridization procedure.

2.9. RNA immunoprecipitation (RIP) assay

RIP assay between UPF1 and HTLV-1 genomic unspliced mRNA was performed following a method described elsewhere [17]. UFP1 was co-immunoprecipitated from the whole cell lysate of MT-2 using goat polyclonal antibody against hUPF1 (Rent-1 (p-14), sc-18260; Santa Cruz Biotechnology, Inc.), and total RNA was extracted from the immunoprecipitant for detection of HTLV-1 genomic unspliced RNA (gRNA) by RT-PCR using primers for the HTLV-1 *gag* region. Immunoprecipitation by a goat polyclonal antibody against GST (GE Healthcare Bioscience) was performed as a negative control. Total RNA from the whole cell lysate (22% vol. of input to immunoprecipitation) was also extracted for RT-PCR of gRNA.

2.10. Statistical analyses

Throughout the present study, two-tailed paired Student's *t*-test was performed to test the statistical difference between the experimental groups. Asterisks in the figures indicate a significant difference between the tested groups (*$p < 0.05$; **$p < 0.01$; and ***$p < 0.001$, $n > 3$).

3. Results

3.1. The cellular UPF1 level influences the turnover rate of HTLV-1 unspliced mRNA

To test the hypothesis that NMD inhibits or antagonizes HTLV-1 replication, the accumulation of genomic primary mRNA was examined in human HeLa cells transfected with an infectious HTLV-1 molecular clone, pFL-MT2 [12], in the presence of the overexpressed key NMD-positive effector, UPF1, or following siRNA-mediated knockdown of UPF1 (Fig. 1A). In the presence of ectopic UPF1, the steady-state level of HTLV-1 genomic unspliced mRNA (gRNA) accumulating from the pFL-MT2 infectious clone significantly decreased, whereas it increased following NMD inhibition by wortmannin treatment or following knockdown with UPF1-specific siRNAs (Fig. 1A). The level of WT-β-globin mRNA, which is not a NMD target, was not significantly influenced by the cellular level of UPF1 or by wortmannin treatment, indicating that the level of HTLV-1 genomic RNA was selectively influenced by cellular NMD activity (Fig. 1A). Reverse-transcriptase (−) PCR with *gag* primers was conducted in all above cDNA samples and it was confirmed that no detectable level of genomic DNA was contaminated in these samples (data not shown). In addition, the viral genomic unspliced RNA was significantly destabilized following UPF1 overexpression in infected cells (half-life = 1.6 h) compared with control cells with endogenous levels of UPF1 (half-life = 3.8 h) (Fig. 1B, left panel). In stark contrast, HTLV-1 unspliced RNA was stabilized after UPF1 knockdown by siUPF1 in infected cells (half-life = 7.9 h) compared to the control cells transfected with the control siRNA (half-life = 2.4 h) (Fig. 1B right panel). In cells, the factors required for NMD activity are often associated with cytoplasmic foci known as processing bodies (P-bodies). Therefore, the subcellular localization of HTLV-1 genomic unspliced RNA was examined in HTLV-1 infected HeLa cells by in situ hybridization and compared with the distribution of Azami-Green labeled de-capping protein 2 (DCP2) protein, which is a known P-body marker. HTLV-1 unspliced RNA (gRNA) was observed throughout the cytoplasm, but a substantial fraction of the RNA co-localized with DCP2 in brightly stained granular centers, suggesting that a significant level of the viral RNA localized to the P-bodies (Fig. 1C). Moreover, immunoprecipitation assays demonstrated that UPF1 is in a complex with HTLV-1 unspliced RNA and the amount of viral RNA interacting with UPF1 depends on the phosphorylation status of UPF1, i.e., phosphorylated UPF1 with okadaic acid treatment interacted with a higher amount of HTLV-1 genomic unspliced RNA (Fig. 1D). These data support the notion that HTLV-1 unspliced RNA is specifically targeted by UPF1 for processing via the NMD pathway.

3.2. HTLV-1 derived reporter activity is NMD sensitive

To further examine the impact of NMD on HTLV-1 RNA stability, a luciferase-based reporter plasmid was constructed (Fig. 2A). The reporter comprises the renilla luciferase ORF fused in-frame with the 5′ end of a HTLV-1 fragment spanning the 3′ end of *gag* through *pro* and into the 5′ end of *pol* (1677–2594 nt). The HTLV-1 sequences are followed at the 3′ end by a β-globin splicing sequence, which is positioned for recruitment of the exon junction complex (EJC) downstream of the HTLV-1 frameshift fragment. Splicing at the correct site, i.e., between exon 2 and exon 3 of β-globin mRNA, has been confirmed by sequencing PCR-amplified transcripts produced from the reporter (data not shown). This reporter provides four possible translation patterns, of which three generate a PTC and are expected to trigger NMD (Fig. 2A). The impact of siRNA knockdown of UPF1 or UPF2, which led to the suppression of NMD activity, on HTLV-1 derived reporter activity was examined in HeLa cells. Of note, the reporter activities increased in HeLa cells treated with siUPF1 and siUPF2 (Fig. 2B). Thus, reporter transcripts spanning 1677–2594 nucleotides of HTLV-1 genomic RNA are stabilized by NMD inhibition and are consequently targeted by NMD.

3.3. NMD activity in HTLV1 transformed cell lines

To determine cellular NMD activity, we employed a luciferase-based β-globin reporter system, which encodes renilla luciferase that is linked to the WT β-globin gene sequence as a control (WT-Glo) or an essentially identical construct but with a PTC-harboring β-globin gene sequence downstream of renilla ORF (PTC-Glo) (Fig. 3A). This β-globin-based reporter provides a robust and reliable readout of cellular NMD activity in HeLa cells (Fig. 3A) and in the T-cell line, Jurkat (Fig. S1).

To determine if cell transformation by HTLV-1 specifically perturbs NMD activity, we tested NMD activity in control HTLV-1-unrelated cell lines (fibroblasts and T cell lines) and in HTLV-1 infected T cell lines. In these assays, the control HTLV-1-unrelated cell lines showed relative NMD activities of >80% of that in control HeLa cells, which have intact NMD activity. In contrast, the NMD values for HTLV-1 infected (i.e., HTLV-1-transformed and ATL-derived) T cell lines were <50% of that observed in control HeLa cells, indicating lower NMD activities (Fig. 3B). These results raised the possibility that NMD is partially suppressed or inhibited in HTLV-1 infected cells and in ATL cells.

3.4. Impact of HTLV-1 infection on NMD activity

To examine whether HTLV-1 infection has any effect on the host cell NMD activity, sHeLa cells, which stably express both firefly-PTC-Glo and renilla-WT-Glo reporter genes, were infected with HTLV-1 by co-cultivation with MT-2 cells. Successful infection of HTLV-1 from MT-2 to sHeLa cells was confirmed by detection of HTLV-1 unspliced mRNAs by semi-quantitative RT-PCR (Fig. 3C). The expression of HTLV-1 unspliced mRNA was evaluated 1–4 days after infection. The highest levels of unspliced RNA were observed during the first 2 days of infection, corresponding to the peak levels of HTLV-1 *tax*/*rex* mRNAs and the Tax and Rex proteins (Fig. 3C). To confirm successful infection in HeLa cells co-cultured with MT-2, the expression pattern of the Tax protein was observed by immunocytochemistry (Fig. S2A). Genomic fingerprinting PCR of the human MCT118 locus in the infected sHeLa cells showed no MT-2-derived bands, confirming that viral proteins detected in the infected sHeLa cells were attributed to HTLV-1

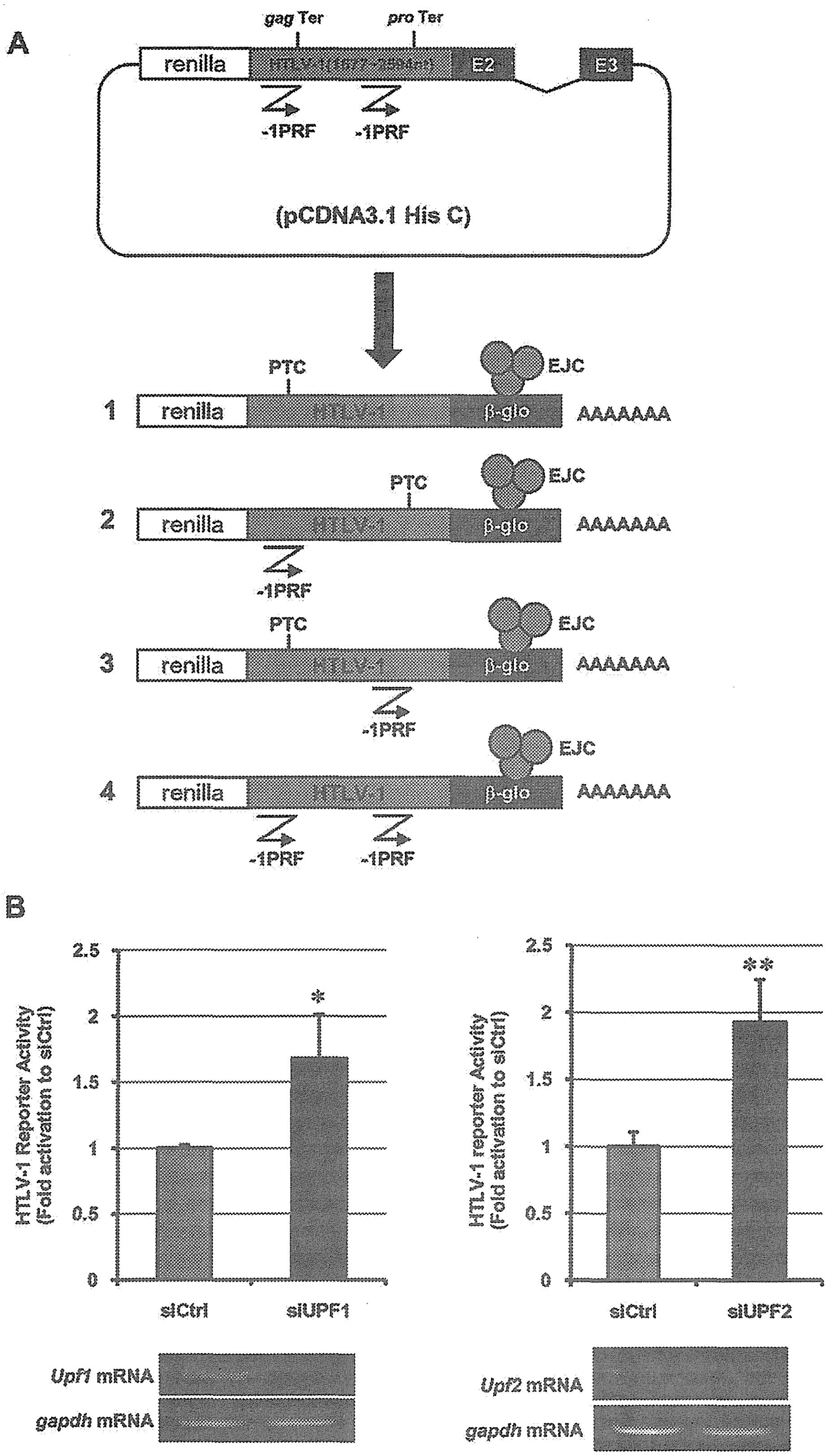

Fig. 2. HTLV-1 derived reporter activity is NMD sensitive. (A) A schematic structure of the HTLV-1 derived reporter plasmid and four possible translation patterns. As indicated, the HTLV-1 fragment in the reporter plasmid contains two −1 PRF signals (shown by ⥵) and 3/4 of these translation patterns result in PTC. (B) The HTLV-1 derived reporter activity was NMD dependent in HeLa cells. The relative HTLV-1 reporter activity was increased by NMD inhibition through siRNA-mediated suppression of UPF1 and UPF2 ($n = 3–5$, mean ± SD; $*p < 0.05$; $**p < 0.01$).

infection but not to contamination of co-cultured MT-2 cells (for genomic fingerprinting PCR, see Supplementary material and methods for more details) (Fig. S2B). NMD activity in these HTLV-I-infected sHeLa cells was significantly suppressed on day 1 ($p < 0.05$) and on day 2 ($p < 0.01$) after infection compared with that in control sHeLa cells co-cultured with uninfected cells (Fig. 3D). These results indicated that HTLV-1 caused a temporal suppression of NMD activity. Of note, the timing of maximum suppression of NMD activity corresponded to the peak expression of HTLV-1 *tax/rex* mRNAs and proteins and correlated with peak accumulation of HTLV-1 unspliced mRNA (Fig. 3C and D). Moreover, co-culture of sHeLa cells with MT-2 in the presence of the reverse transcriptase inhibitor azidothymidine (AZT) resulted in a dose-dependent rescue of NMD activity, supporting the idea that the suppression of NMD activity is indeed caused by HTLV-1 infection of target sHeLa cells and that this suppression requires reverse transcription and provirus integration (Fig. 3E).

3.5. HTLV-1 Rex is the principal viral factor inhibiting host NMD activity

Next, we examined HTLV-1 gene products for the ability to suppress host NMD activity. The relative NMD activity in sHeLa cells that ectopically express p27Rex (Rex), p21Rex, p30II, and Tax was analyzed using the dual-luciferase NMD reporter assay at 24,36, and 48 h after transfection. As shown in Fig. 4A, NMD activity was significantly suppressed 24 h after transfection when p27Rex or p21Rex was expressed. In these experiments, the HTLV-1 transcriptional transactivator Tax was also found to inhibit NMD activity, but this effect was consistently less than that observed for p27Rex or p21Rex.

The most significant impact on host NMD activity was the dose-dependent suppression exerted by p27Rex and to a slightly lesser degree, p21Rex (Fig. 4B). Of note, NMD reporter constructs do not contain sequences corresponding to the highly structured RxRE. Consequently, we suggest that the suppression of NMD activity by Rex is not due to RxRE-dependent and Rex-mediated nuclear export of unspliced mRNAs. Indeed, nuclear export of unspliced β-globin mRNA, transcribed from the reporter plasmid, was not enhanced by Rex (Fig. S3A). We also confirmed that insertion of RxRE after the β-globin sequence of the NMD reporter plasmid did not exhibit any significant influence on Rex-induced NMD inhibition (Fig. S3B). Moreover, our study demonstrated that p21Rex, which lacks the N-terminal RxRE-binding domain, also exhibited NMD inhibitory activity, supporting the view that NMD inhibition is due to a genetically separable aspect of Rex function that is independent of the arginine-rich RxRE-binding motif. Other HTLV-1 accessory proteins, such as p12, p13, and antisense-encoded HBZ, did not show any significant influence on the cellular NMD activity (Fig. S4).

3.6. Rex inhibits global NMD activity of the cell

On confirmation that Rex stabilizes chimeric NMD reporter mRNA, we tested if Rex stabilizes endogenous NMD target mRNA. Fig. 5 shows the decay rates of NMD target mRNAs in CEM cells stably expressing Rex or in control cells showing no Rex expression. The selected mRNAs contained uORFs (MAP3K14, IL6, DUSP10, Fyn, PTPRF, ARHGEF18, and ASNS) or 3′ UTR intron (DEXI) as NMD-inducing features and stabilization under UPF1 knockdown was confirmed (MAP3K14, PTPRF, ARHGEF18, and ASNS) or expected (DUSP10, Fyn, IL6, and DEXI) by Mendell et al. [2]. The graphs show that these mRNA substrates for NMD are significantly stabilized by Rex overexpression in a T cell line. These NMD target mRNAs were specifically stabilized in CEM-Rex, since the stability of β-actin mRNA, a non-NMD target, was almost the same between CEM-empty and CEM-Rex when the stabilities of β-actin mRNA and NMD target mRNA were separately illustrated (data not shown). These results provide strong evidence that Rex serves as a general inhibitor of NMD.

3.7. NMD inhibition by Rex enhances HTLV-1 expression

Finally, we examined the effects of p27Rex, p21Rex, p30II, and Tax on HTLV-1 derived reporter activity. As shown in Fig. 6A, p27Rex significantly increased HTLV-1 reporter activity, which was very similar to that following NMD inhibition by siUPF1 or siUPF2 (Fig. 2B). p21Rex also significantly elevated HTLV-1 reporter activity, but to a lesser extent compared with p27Rex, whereas p30II and Tax did not significantly influence reporter activity (Fig. 6A). As anticipated from the accrued data and early reports by others [18–20], we also demonstrated that unspliced HTLV-1 mRNA was significantly stabilized in cells containing p27Rex (half-life = 11.3 h) compared with control cells containing empty vectors (half-life = 2.3 h) (Fig. 6B). On the other hand, p30II and Tax did not show significant effects on stabilization of unspliced HTLV-1 mRNA (half-lives = 3.4 h and 2.8 h, respectively). Interestingly, p21Rex, which does not have NLS and hence does not localize to the nucleus, also stabilized unspliced HTLV-1 unspliced mRNA (half-life = 11.0 h). These data further support that stabilization of viral genomic RNA by Rex is, at least partially, achieved by its function in the cytoplasm. Significantly, viral particle production, as determined by HTLV-1 Gag p53 (precursor), p24, and p19 protein expression levels, was increased under conditions of NMD inhibition by antisense-*upf2* mRNA overexpression that suppressed UPF2 protein expression (Fig. 6C). In addition, this increased level of Gag protein, especially in p53 and p19, was comparable to that observed following p27Rex and p21Rex overexpression (Fig. 6D). Given that p27Rex and p21Rex significantly stabilizes HTLV-1 *gag* mRNA (Fig. 6B), these data suggest that Rex enhances HTLV-1 replication by stabilizing unspliced viral transcripts via the suppression of host NMD activity.

4. Discussion

In this study, we demonstrate that HTLV-1 genomic and *gag/pol* RNA is recognized by UPF1, the principal regulator and initiator of NMD, and is thereby targeted for destruction

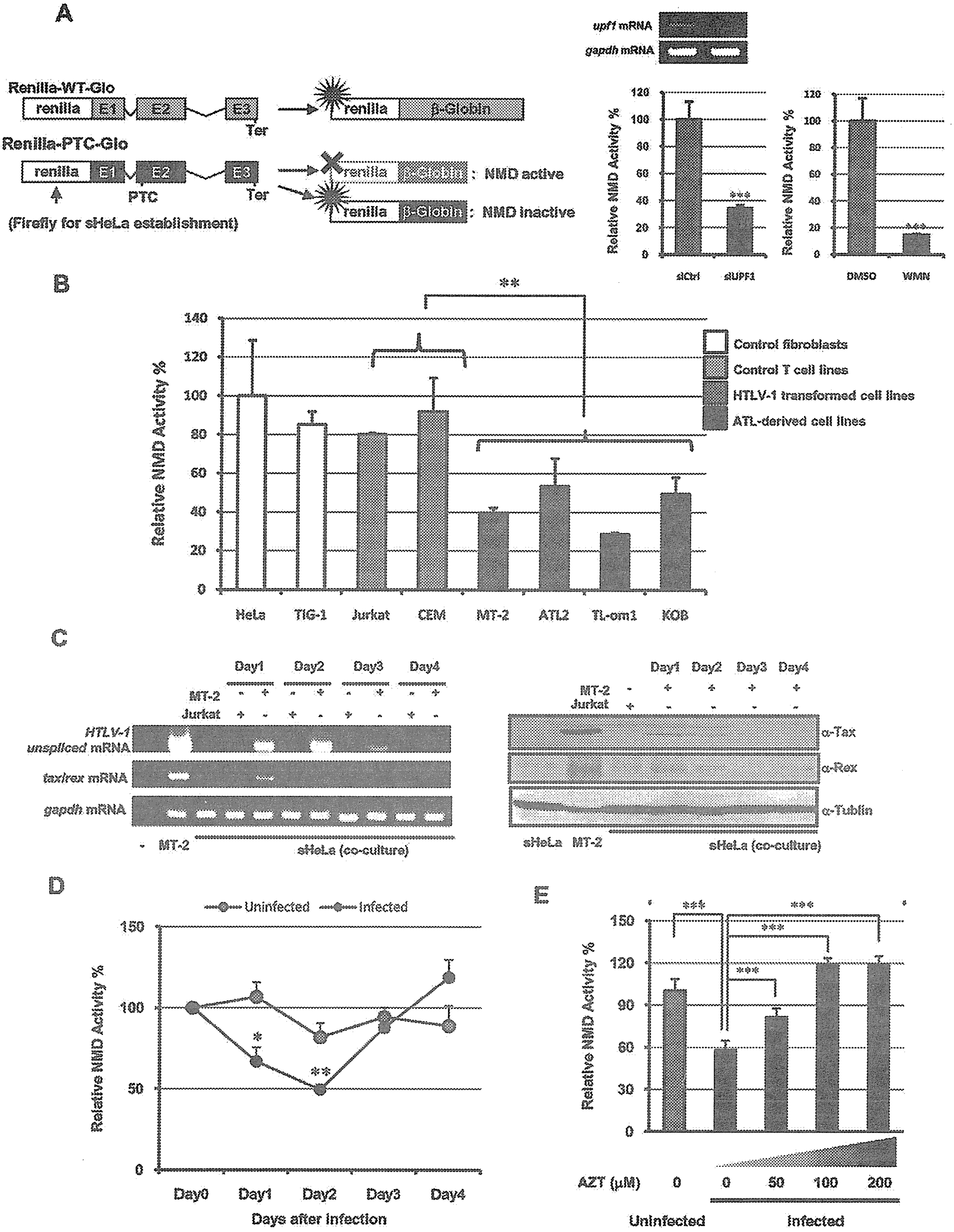

Fig. 3. HTLV-1 infection inhibits cellular NMD activity. (A) A schematic representation of the β-globin NMD reporter plasmids. PTC indicates a premature termination codon and Ter indicates a WT stop signal. The renilla fragment of Renilla-PTC-Glo was replaced with the firefly fragment for establishment of sHeLa cells, which stably expressed both Renilla-WT-Glo and Firefly-PTC-Glo, thus WT-Glo and PTC-Glo expression level was detected as renilla and firefly luciferase activity, respectively. ✹ indicates the luciferase activity. The renilla activity of Renilla-WT-Glo is always active and not influenced by the cellular NMD activity.

by the host NMD machinery. Moreover, we found that HTLV-1 has evolved mechanisms to override and escape the host NMD pathway. We provide evidence that HTLV-1 Rex plays a critical role in the suppression of host NMD activity.

Firstly, we demonstrated that the host-encoded NMD specifically targets HTLV-1 genomic RNA and primary transcripts for RNA turnover. Therefore, host NMD acts to reduce viral structural gene expression and perturbs virus production. The steady-state expression of HTLV-1 unspliced mRNA showed a negative correlation with cellular NMD activity (Fig. 1A), and the stability of unspliced viral mRNA was highly sensitive to cellular NMD activity (Fig. 1B). Luciferase reporter assays, in which the luciferase activity reflects the stability of a *gag*-derived fragment of HTLV-1 genomic RNA, showed that the stability of HTLV-1 *gag* mRNA was directly influenced by the cellular level of UPF1 or UPF2, the key positive regulator of NMD (Fig. 2). Many researchers have demonstrated that UPF1 phosphorylation by the serine/threonine kinase SMG1 facilitates triggering of NMD and exclusion of aberrant mRNAs from the normal translational pathway. These mRNAs are redirected to the P-body, where they await targeted turnover [21,22]. UPF1 plays an important role in discrimination of PTCs that are positioned upstream of EJC at the last exon–exon boundary of spliced mRNAs and selectively activates the NMD machinery for degradation of the targeted mRNA [23]. Recognition of PTC by UPF1 is achieved by interaction of UPF1 at the termination codon with UPF2/UPF3 at EJC, which becomes possible only when a termination codon is positioned upstream of EJC. In yeast, the P-body is the major site for PTC-containing aberrant mRNAs awaiting degradation [24–26]. In mammalian and human cells, all NMD components localize to P-bodies [21] and phosphorylated UPF1 accumulates at these structures [22], supporting the notion that P-bodies accumulate mRNAs targeted for NMD turnover in mammalian cells. Taken together, accumulating evidence indicates that UPF1 is the key regulator in discrimination, selection, and translocation of aberrant mRNAs to P-bodies where they await degradation [21–23,26,27]. The results in the present study demonstrate that phosphorylated UPF1 interacts with HTLV-1 unspliced RNA with a high affinity and the HTLV-1 unspliced RNA complex accumulates in P-bodies (Fig. 1C and D). Our results thus indicate that HTLV-1 genomic RNA is detected by UPF1 as are other cellular NMD target mRNAs and transferred to P-bodies for degradation. Consistent with this notion, NMD antagonized efficient HTLV-1 replication (Fig. 1A and B), whereas the suppression of NMD activity led to a significant increase in HTLV-1 Gag proteins, p53, p24, and p19 (Fig. 6C). Thus, NMD destabilizes HTLV-1 genomic RNA and reduces the expression of viral structural proteins, presumably leading to a reduction in viral particle formation.

Several reports raise the possibility that retroviral transcripts are selectively targeted by the host mRNA decay mechanism, and they have unique or overlapped strategies to avoid degradation. Viral mRNAs of Rous sarcoma virus (RSV) [28] and human foamy virus [29] are selectively degraded in the host cell, although the authors of those studies concluded that the degradation may be accomplished by pathways distinct from NMD. Ajamian et al. reported influence of host encoded NMD-factor, UPF1, on unspliced HIV-1 mRNA, intriguingly enhancing the stability of HIV-1 mRNA [30]. Hogg and Goff proposed a possible model that 3′ UTR-length-dependent accumulation of UPF1 functions as a mark of potential mRNA-decay target [31]. The authors speculated that retroviruses may take advantage of this host-encoded system by employing in-frame read though and/or frame-shifting, which prevents steady-state UPF1 interaction and RNP composition, thus disrupts recognition of the viral mRNA as a decay target. In addition to these previous reports, our data show that unspliced HTLV-1 RNA is a target of a powerful host-encoded mRNA decay mechanism, NMD, and for efficient replication and propagation of new viral particles, it is critical for HTLV-1 to evade the NMD pathway.

On confirming that the host NMD pathway represents a significant impediment to efficient HTLV-1 replication, we posed the critical question: has HTLV-1 evolved a strategy to evade NMD? We observed that HTLV-1-infected cell lines have significantly lower basal NMD activities than HTLV-1-unrelated cell lines (Fig. 3B), implying that HTLV-1 infection may influence host NMD activity. Indeed, the NMD activity was notably suppressed by HTLV-1 infection or protected by inhibition of HTLV-1 infection via AZT treatment (Fig. 3C–E), suggesting the existence of viral factor(s) that suppress the host NMD pathway. Besides the structural proteins, HTLV-1 encodes regulatory and accessory proteins (Tax, Rex, p30II, p12, and p13) in the pX region of the genome. The functions of those proteins have been well studied and reviewed [32,33]. Tax is a multifunctional oncoprotein and transcriptional transactivator that regulates both viral and cellular gene expression [34,35]. HTLV-1 Rex is a virus-encoded, high-affinity, RNA-binding protein that binds

On the other hand, the luciferase activity of PTC-Glo, of which transcript is NMD target, can be detected only under NMD inhibition. The reporter is sensitive to changes in NMD activity in HeLa cells (right panel). Data from three independent experiments are shown ($n = 3$, mean ± SD; $^{***}p < 0.001$). (B) NMD activities were measured by β-globin-based NMD reporter assays in control fibroblasts (HeLa and TIG-1), control T-cell lines (Jurkat and CEM), HTLV-1-transformed cell lines (MT-2 and ATL2), and ATL-derived cell lines (TL-Om1 and KOB). HTLV-1-infected T cell lines show significantly lower NMD activities compared with HTLV-1-unrelated cell lines. Data from three independent experiments are shown ($n = 3$, mean ± SD; $^{**}p < 0.01$). (C) The course of HTLV-1 expression in sHeLa cells co-cultured with MT-2. *Gag* or *tax/rex* mRNA by RT-PCR (left panel) as well as Tax and Rex protein levels determined by Western blotting (right panel) show peaked viral expression 1 and 2 days after infection. (D) NMD activity was measured via dual luciferase assays in HTLV-1 infected sHeLa cells and compared with that in uninfected control cells. Gray circles indicate the results from uninfected control cells, while black circles represent data from HTLV-1 infected cells. Significant NMD inhibition was observed on the first ($p < 0.05$) and second ($p < 0.01$) days after HTLV-1 infection. Results shown are from three independent experiments ($n = 3$, mean ± SE; $^{*}p < 0.05$; $^{**}p < 0.01$). (E) NMD inhibitory effect of HTLV-1 infection is diminished by AZT treatment in HTLV-1 infected sHeLa cells by co-cultivation with MT-2 cells. NMD inhibition by HTLV-1 was abrogated in a dose-dependent manner by AZT treatment ($n = 6$, mean ± SD; $^{***}p < 0.001$).

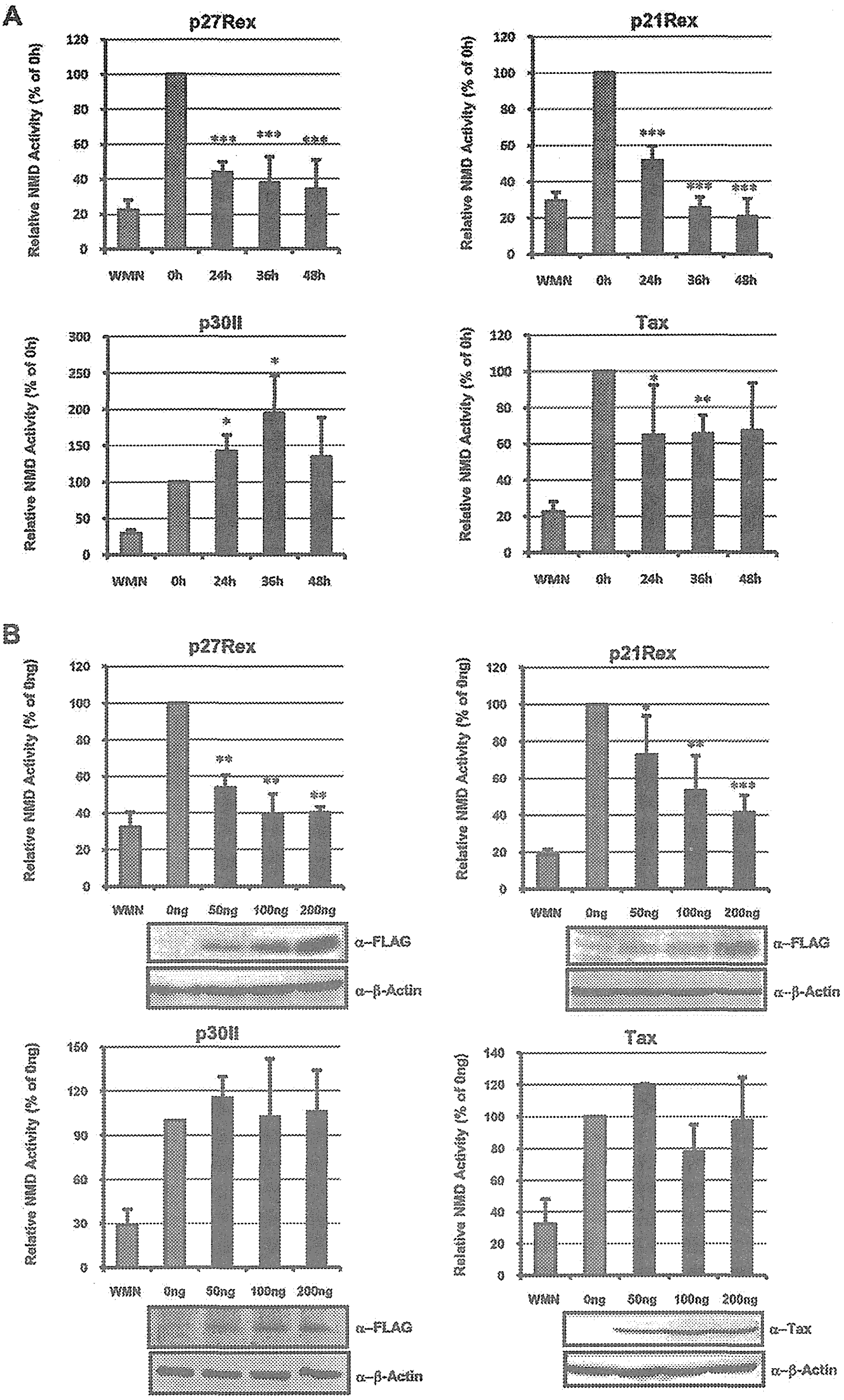

Fig. 4. HTLV-1 Rex is the key viral factor inhibiting NMD. (A) p27Rex and p21Rex inhibit NMD activity in a time-dependent manner, when 200 ng each of viral protein expression plasmid was transfected to sHeLa cells. Tax also demonstrated an NMD inhibitory effect but to a less significant level compared with p27Rex and p21Rex. A representative result from three independent experiments is shown ($n = 3$, mean ± SD; $*p < 0.05$; $**p < 0.01$; $***p < 0.001$). (B) Both p27Rex and p21Rex suppressed NMD activity in a dose-dependent manner when 50–200 ng of viral protein expression plasmid was transfected to sHeLa cells. A representative result from three independent experiments is shown ($n = 3$, mean ± SD; $*p < 0.05$; $**p < 0.01$; $***p < 0.001$).

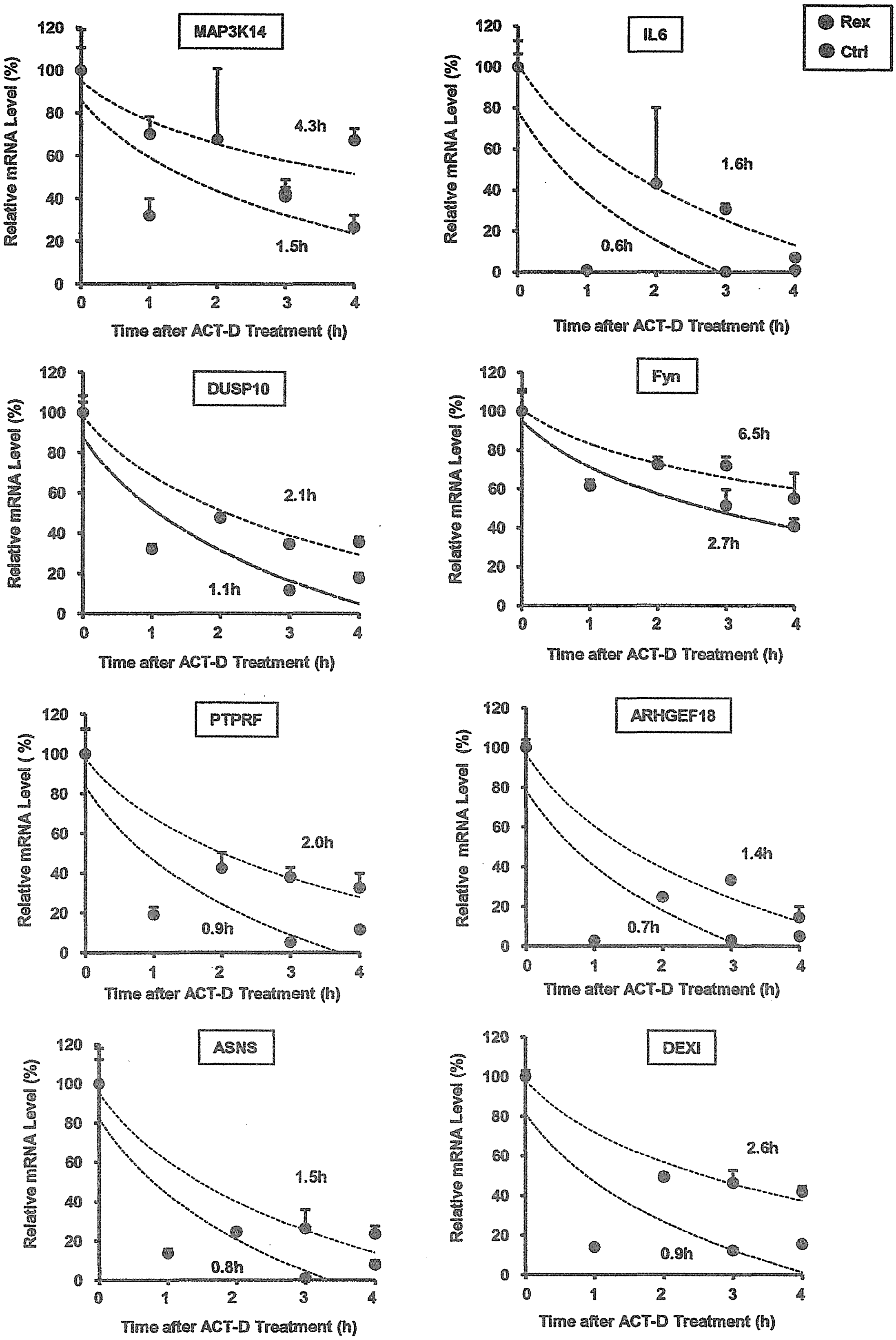

Fig. 5. Rex inhibits global NMD activity. The stability of NMD target mRNAs containing uORFs or 3′ UTR introns as NMD-inducing features [2] were measured in CEM-Rex and CEM-Ctrl. These mRNAs for NMD substrates were significantly stabilized in Rex-overexpressing cells, indicating that Rex represents a general block to global cellular NMD activity. Red circle: CEM-Rex; black circle: CEM-Ctrl. The indicated time is the half-life of tested mRNA calculated based on the regression curve (dashed line).

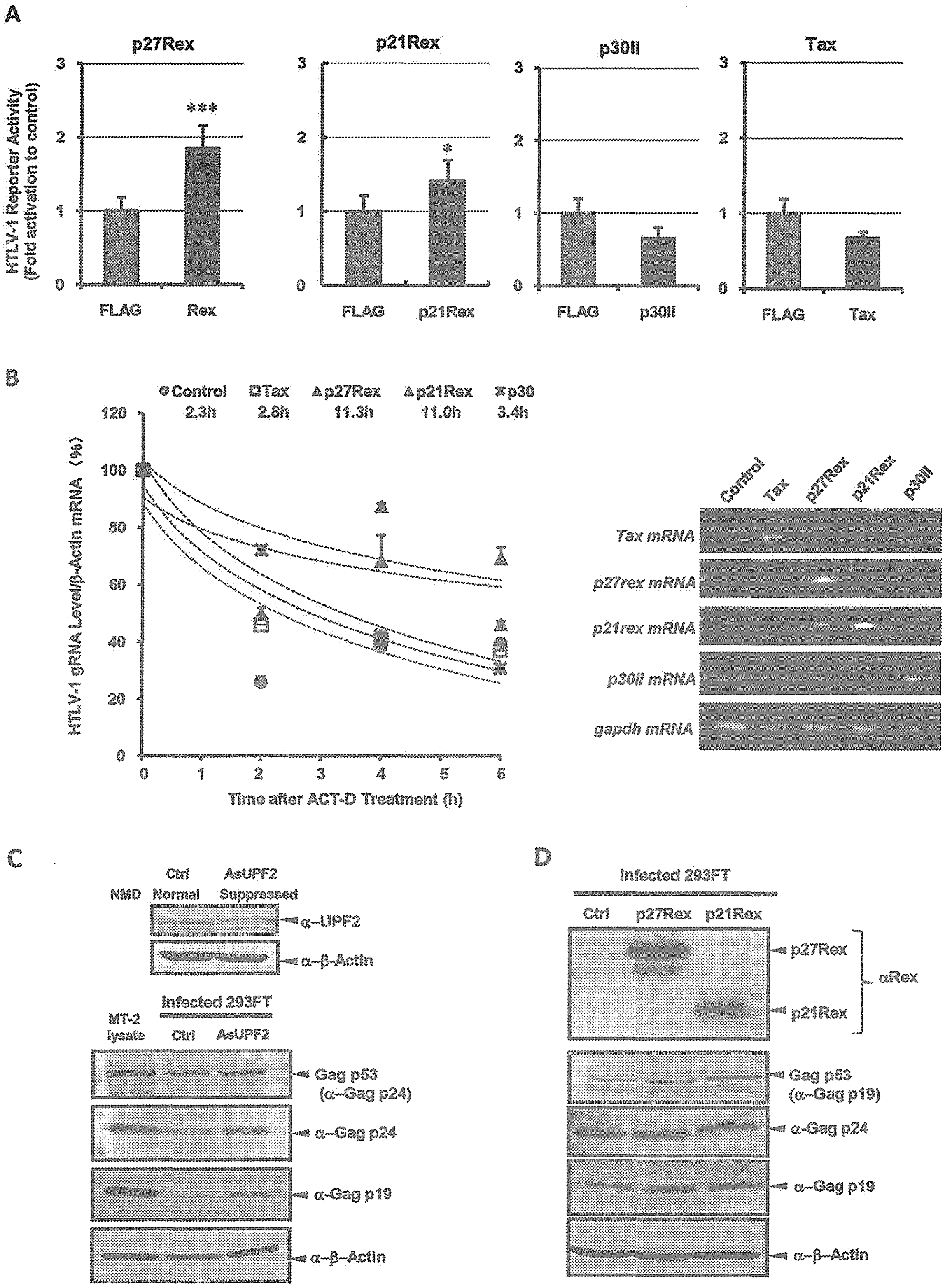

Fig. 6. Rex stabilizes HTLV-1 unspliced mRNA and enhances viral replication via NMD inhibition. (A) The effects of p27Rex, p21Rex, p30II, and Tax on HTLV-1 derived reporter activity in HeLa cells. The reporter activity was significantly increased by p27Rex and p21Rex but not by p30II and Tax ($n = 3$–5, mean ± SD; $*p < 0.05$; $***p < 0.001$). (B) The effect of HTLV-1 regulatory proteins p27Rex (red ▲), p21Rex (purple ▲), p30II (black×), Tax (blue □), and control (green ●) on the stability of HTLV-1 genomic unspliced RNA in HTLV-1 infected HeLa cells by co-cultivation with MT-2 cells. HTLV-1 unspliced RNA in p27Rex-overexpressing cells was significantly stabilized (half-life = 11.3 h), followed by stabilization in p21Rex-overexpressing cells (half-life = 11.0 h) compared